

## **Gas-particle partitioning of pesticides in the atmosphere of the North China Plain**

Liping Guo<sup>1</sup>, Shuping Shi<sup>1</sup>, Ying Li<sup>2</sup>, Martin Brüggemann<sup>3</sup>, Mingyu Zhao<sup>1</sup>, Hongyu Mu<sup>1</sup>,

Daniel M. Figueiredo<sup>4</sup>, Junxue Wu<sup>5</sup>, Kai Wang<sup>1</sup> \*

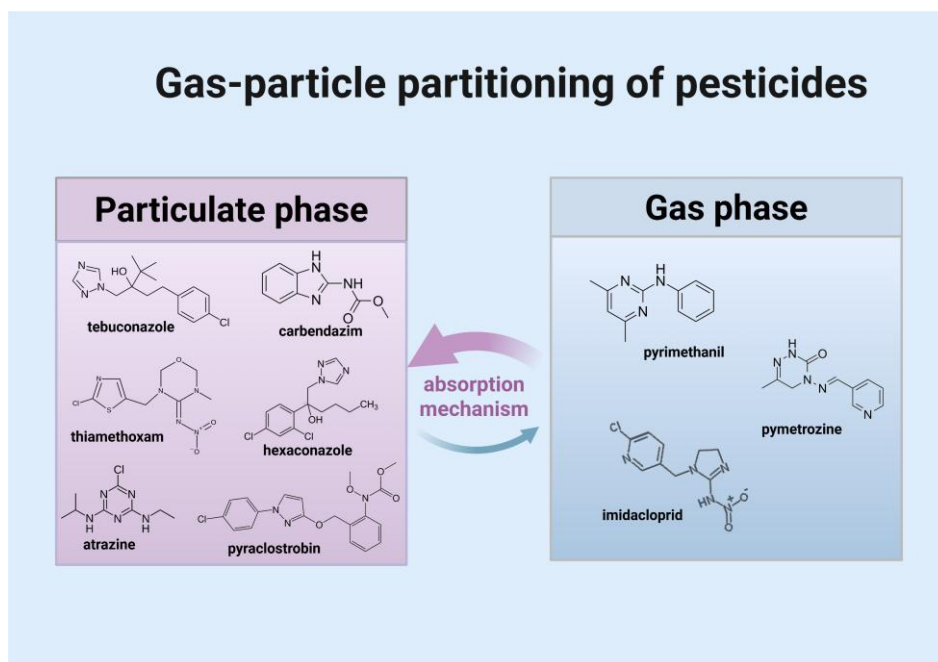
<sup>1</sup> State Key Laboratory of Nutrient Use and Management, College of Resources and Environmental Sciences; National Academy of Agriculture Green Development; Key Laboratory of Plant-Soil Interactions of Ministry of Education, National Observation and Research Station of Agriculture Green Development (Quzhou, Hebei), China Agricultural University, Beijing 100193, PR China, <sup>2</sup> Key Laboratory of Industrial Ecology and Environmental Engineering (Ministry of Education), School of Environmental Science and Technology, Dalian University of Technology, Dalian 116024, China, <sup>3</sup> Bayer AG, Crop Science Division, R&D, Environmental Safety, Monheim, Germany, <sup>4</sup> Institute for Risk Assessment Sciences, Utrecht University, 3584 CM Utrecht, Netherlands, <sup>5</sup> Institute of Plant Protection, Beijing Academy of Agriculture and Forestry Science, Beijing 100097, China

**Corresponding Author:** Kai Wang, Email: [kaiwang\\_ly@cau.edu.cn](mailto:kaiwang_ly@cau.edu.cn)

1 **Abstract:** Pesticide residues are ubiquitous in the atmosphere in the North China Plain (NCP),  
2 with concentrations largely determined by application patterns and physicochemical parameters  
3 such as persistence and volatility. However, knowledge of gas-particle partitioning of pesticides  
4 remains limited, hindering a comprehensive understanding of their abundance, transport, and  
5 health risks. Here, we aim to elucidate the underlying mechanism of gas-particle partitioning  
6 for pesticides. In this study, 14 pairs of air and particulate matter samples were collected  
7 simultaneously in Quzhou County, the NCP. A total of 19 pesticides were observed in both gas  
8 and particulate-phases. Average pesticide concentrations in particulate phase ( $2025.76 \pm$   
9  $1048.83 \text{ pg/m}^3$ ) were significantly higher than in gas phase ( $143.38 \pm 146.31 \text{ pg/m}^3$ ),  
10 accounting for 93.4% of the total atmospheric pesticide mass. Tebuconazole ( $662.49 \pm 448.52$   
11  $\text{pg/m}^3$ ), pyraclostrobin ( $212.01 \pm 119.70 \text{ pg/m}^3$ ), and carbendazim ( $158.68 \pm 86.54 \text{ pg/m}^3$ )  
12 exhibited the highest concentrations in the particulate phase, whereas pyrimethanil ( $93.00 \pm$   
13  $79.18 \text{ pg/m}^3$ ), pymetrozine ( $22.96 \pm 21.50 \text{ pg/m}^3$ ), and imidacloprid ( $5.78 \pm 2.64 \text{ pg/m}^3$ )  
14 were predominant in the gas phase. A positive correlation between temperature and particulate-  
15 phase pesticide concentrations was found, as indicated by rising of  $\log K_p$  values which is likely  
16 attributable to an interplay of pesticide physicochemical properties, ambient relative humidity,  
17 particle phase state and pesticide use patterns. Gas-particle partitioning model simulations  
18 showed absorption as the main mechanism of gas-particle partitioning, indicating atmospheric  
19 pesticides are absorbed into the interior organic film of particulate matter.

20  
21 **Keywords:** Atmospheric pesticide, Gas-particle partitioning, Influence factor, the North  
22 China Plain

28 **Graphic Abstract:**



29  
30  
31  
32

33 **1 Introduction**

34 Pesticides have been widely applied worldwide against pests in agriculture since  
35 dichlorodiphenyltrichloroethane (DDT) was discovered to have insecticidal properties in 1939  
36 (Turusov et al., 2002). Pesticides play an important role in the development of agriculture by  
37 increasing the yield of agricultural products and improving their quality (Aktar et al., 2009).  
38 Pesticide usage in China reached 229,026 metric tons in 2023, accounting for around 6.14% of  
39 global pesticide use (FAO, 2025). However, the pesticide utilization rate (the proportion of the  
40 pesticide deposited on the target per unit area to the total amount of pesticide used) for the three  
41 major cereal crops (i.e., wheat, maize and rice) in China was only about 41% (China, 2021)  
42 meaning that more than half of the pesticides were not effectively absorbed by the target crops  
43 or pests and was instead lost to the environment (e.g., water, soil and atmosphere) (Tudi et al.,  
44 2022). While the fate of pesticides in soil and water has been studied extensively over the last

45 decades, their behavior, distribution, and degradation in the atmosphere have only recently  
46 gained increasing interest (Brüggemann et al., 2024). There are mainly three ways for pesticides  
47 to enter the atmosphere: drift, volatilization, and wind erosion. In detail this means that a portion  
48 of applied pesticides reaches the atmosphere directly during application (e.g. spray drift and  
49 vapor drift) (van den Berg et al., 1999). Later, after application, soil particles that have adsorbed  
50 pesticides may serve as a reservoir and release residues into the atmosphere through  
51 resuspension of soil particles, also referred to as wind erosion (Glotfelty et al., 1989).  
52 Furthermore, pesticides may volatilize from plants, soil, surface water, and the surfaces of old  
53 industrial sites under the influence of diffusive air-surface mass exchange (Cabrerizo et al.,  
54 2011). [Atmospheric pesticides have been monitored globally. Yera and Vasconcellos analyzed](#)  
55 [concentrations of pesticides such as atrazine in the atmosphere of the São Paulo region, Brazil,](#)  
56 [ranging from 17–210 pg m<sup>-3</sup> \(Yera et al., 2021\). In Costa Rican banana plantations, Karla et al.](#)  
57 [\(2026\) reported that the highest concentrations of the detected pesticides were for pyrimethanil](#)  
58 [\(34.3 ng/m<sup>3</sup>\), followed by fenpropidin \(9.0 ng/m<sup>3</sup>\) and terbufos \(8.4 ng/m<sup>3</sup>\). Tian et al. \(2021\)](#)  
59 [conducted observational analysis and quantification of organochlorine pesticides in the](#)  
60 [atmosphere across nine cities in the Pearl River Delta region of China, finding that](#)  
61 [concentrations of 16 organochlorine pesticides in summer \(0.33–1431 pg m<sup>-3</sup>\) were higher than](#)  
62 [0.26–893 pg m<sup>-3</sup> in winter. In a study on the North China Plain \(NCP\), ten organochlorine](#)  
63 [pesticides with concentrations ranging from 11.67 to 865.60 pg m<sup>-3</sup> were observed in](#)  
64 [atmospheric PM<sub>2.5</sub> in a rural area of Baoding City, Hebei Province \(Sun et al., 2020\). Another](#)  
65 [long-term monitoring study identified chlorpyrifos, carbendazim, and atrazine as the pesticides](#)  
66 [with the highest detection rates \(≥87%\) in the NCP, with annual concentrations ranging from](#)

67 [1.71 to 16.05 pg m<sup>-3</sup> \(Zhao et al., 2023\).](#)

68 Upon entering the air, gas-particle partitioning occurs between the gas phase and particulate  
69 phase depending on the physicochemical properties of the pesticides (e.g., vapor pressure,  
70 octanol-air partition coefficient,  $K_{oa}$ ), the concentrations of total suspended particulate matter  
71 (TSP) and meteorological parameters (ambient temperature and relative humidity). Among  
72 these factors, vapor pressure ( $V_p$ ) is widely acknowledged as the main factor determining the  
73 effective volatilization rates. Pesticides with  $V_p$  (at 20 °C) higher than  $1 \times 10^{-2}$  Pa are  
74 predominantly present in the gas phase, while those with  $V_p$  below  $1 \times 10^{-5}$  Pa can be seen as  
75 completely present in the particulate phase (Yusà et al., 2009). The conventional Junge-Pankow  
76 model attributes ~~gas-particle partitioning~~[particle/gas partitioning](#) to surface adsorption, whereas  
77 the absorption model assumes that chemicals dissolve into particles coated by organic films  
78 (Harner and Bidleman, 1998). Since most pesticides are semi-volatile compounds with  
79 moderate vapor pressure, they are distributed in both the gas phase and particulate phase (Bedos  
80 et al., 2002; Wang et al., 2024). Pesticides in the gas phase can be directly absorbed into the  
81 lungs and participate in the blood circulation, potentially causing adverse effects on the  
82 cardiovascular system and almost all organs (Ngo et al., 2010). The pesticides in fine particulate  
83 matter are able to penetrate deeply into the respiratory system, causing a spectrum of health  
84 hazards (Woodrow et al., 2019). These pesticides have the potential to affect various systems,  
85 such as the respiratory, circulatory, immune, and endocrine systems, and may even contribute  
86 to carcinogenesis (Kaur et al., 2019). A previous study demonstrated that the half-lives in  
87 particulate phase of difenoconazole, tetraconazole, fipronil and 8 other pesticides were longer  
88 than the estimated half-lives in the gas phase allowing them to travel longer distances (Socorro

89 et al., 2016). Because of the different behavior and effects of gas-phase and particulate-phase  
90 pesticides on human health and the environment, it is of great significance to study the gas-  
91 particle partitioning of atmospheric pesticides for further analysis of their health and  
92 ecotoxicological effects (Brüggemann et al., 2024).

93 In recent years, studies on the gas-particle partitioning of pesticides in the atmosphere mainly  
94 focused on traditional pesticides, such as organochlorine pesticides (Qiao et al., 2019). Sanli et  
95 al. studied the partitioning of organochlorine pesticides in gas phase and particulate phase at a  
96 semi-rural site in Bursa, Turkey, suggesting that the maximum annual mean gas-phase  
97 organochlorine pesticides concentration was  $\beta$ -hexachlorocyclohexane ( $\beta$ -HCH) with 176  
98  $\text{pg}/\text{m}^3$  while the maximum concentration in the particulate phase was  $\beta$ -Endosulfan at 67  $\text{pg}/\text{m}^3$   
99 (Sanlı and Tasdemir, 2020). However, due to their long lifetime in the environment, most of  
100 these pesticides are now prohibited in most countries. In contrast, modern substances exhibit  
101 significantly shorter degradation times in the environment. Still, data on gas-particle  
102 partitioning of such current-use pesticides are rarely available. Wang et al. measured the  
103 atmospheric concentrations of 36 current-use pesticides in gas phase and particulate phase  
104 samples in the Great Lakes basin and analyzed their gas-particle partitioning, suggesting that  
105 chemicals in particulate phase like metolachlor were negatively correlated with relative  
106 humidity (Wang et al., 2021). Nevertheless, there is limited evidence on the mechanism of  
107 pesticides gas-particle partitioning, which hinders our understanding of the atmospheric fate,  
108 transport and health risks of pesticides. Therefore, it is necessary to further research and  
109 understand the gas-particle partitioning of pesticides in the atmosphere.

110 [Quzhou County is a typical agricultural county in the NCP, located in the northeastern part of](#)

111 Handan City, Hebei Province (geographical coordinates: 36°35'43"–36°57'56"N, 114°50'22"–  
112 115°13'27"E; Yu et al., 2021). The total crop planting area in Hebei Province was around 8  
113 million hectares with the pesticide usage of approximately 50,000 tons in 2023 (Hebei  
114 Provincial Bureau of Statistics, 2024). The pesticide utilization rate in Hebei Province is  
115 approximately 30%, which is lower than 50–60% observed in developed countries (Skevas et  
116 al., 2014). Given its representative agricultural setting in the NCP, Quzhou County serves as an  
117 ideal location for investigating the gas–particle partitioning of atmospheric pesticides in the  
118 NCP, thereby contributing to a more comprehensive understanding of pesticide distribution  
119 across the NCP.~~Quzhou County is located in the center of the North China Plain (NCP), which~~  
120 ~~is the region with the highest degree of intensive farming in China. As a typical agricultural~~  
121 ~~county in the NCP situated in the northeast of Handan City, Hebei Province, at geographical~~  
122 ~~coordinates of 36°35'43"–36°57'56"N, 114°50'22"–115°13'27"E (Yu et al., 2021), Quzhou~~  
123 ~~serves as an ideal location for investigating gas–particle partitioning of atmospheric pesticides,~~  
124 ~~facilitating a more comprehensive understanding of pesticide distribution within the NCP.~~(Feng  
125 et al., 2022). This study attempts to (1) analyze the concentrations of atmospheric pesticides in  
126 both gas and particulate phases; (2) assess the effect of meteorological factors on pesticide  
127 concentrations in the atmosphere, and (3) investigate gas-particle partitioning mechanisms  
128 using three different partitioning prediction models.

## 129 **2 Materials and Methods**

### 130 **2.1 Air sampling**

131 A high-volume air sampler (Sibata Scientific Technology Ltd, 080130-1203) fitted with a  
132 polyurethane foam plug (PUF, 90 mm in diameter × 50 mm in thickness) and a quartz fiber

133 filter (QFF, 203 mm × 254 mm, pore size <0.3 μm) was used to capture pesticides in the gas  
134 phase and particulate phase (i.e. TSP), respectively. [Air is first directed through the QFF for the](#)  
135 [collection of TSP, and subsequently through the PUF sampler for the collection of gaseous](#)  
136 [pesticides.](#) Air samples were collected with a sampling period of 7 days (168 hours) at a flow  
137 rate of 150 L min<sup>-1</sup> from February 17<sup>th</sup> to May 20<sup>th</sup> in 2023 at the Quzhou Experiment Station  
138 (36°78'01"N, 114°94'51"E, 40 m above sea level) in Quzhou County, the NCP. Detailed  
139 sampling information is provided in Table S1. In total, 14 gas phase samples and 14 particulate  
140 phase samples were collected. All samples were kept at -20°C until analysis. Meteorological  
141 data (Table S2), including temperature, atmospheric pressure, precipitation, relative humidity,  
142 and wind speed, along with particulate matter (PM<sub>10</sub> and PM<sub>2.5</sub>) concentrations, were obtained  
143 from the Air Quality Monitoring Platform of Handan City  
144 (<http://111.62.17.169:8083/index.html#/map/HomeTianMap>) and the Quzhou Experimental  
145 Station. The mass of TSP was measured by gravimetry.

## 146 **2.2 Sample treatment and instrumental analysis**

147 The PUFs and QFFs were extracted with ultrasound-assisted extraction for 1 hour with a 100  
148 mL mixture of hexane and dichloromethane (1:1, v-v). The extracts (80 mL) were collected in  
149 flat-bottomed flasks and then concentrated to dryness using a rotary evaporator. Next, 1 mL  
150 acetonitrile was added to each flat-bottomed flask and transferred to the centrifuge tube after  
151 sonication, with this process repeated twice. After concentration, the extracts were subsequently  
152 purified on C<sub>18</sub> SPE cartridges and the columns were eluted with 5 mL of acetonitrile. All  
153 fractions were rotary evaporated to dryness and adjusted to a volume of 800 μL with acetonitrile.  
154 Finally, they were vortexed using a vortex oscillator and filtered with syringe filters and

155 transferred to vials for detection.

156 Target analytes in this study included 17 fungicides, 4 herbicides, and 17 insecticides for a total  
157 of 38 compounds purchased from Alta Scientific Co., Ltd (Tianjin, China) (Table S3). [The](#)  
158 [selection of these 38 pesticides is based on their high detection frequency in both gas and](#)  
159 [particulate phases, as reported in previous studies conducted in the North China Plain by Zhao](#)  
160 [et al. \(2023\) and Mu et al. \(2022\).](#) All solvents and chemicals used in this study were of high-  
161 performance liquid chromatography (HPLC) grade or higher. A Waters ACQUITY TQD ultra-  
162 high performance liquid chromatography system coupled with a triple-quadrupole mass  
163 spectrometer (UHPLC-MS/MS) was used to analyze the pesticides. The chromatographic and  
164 mass spectrometric conditions were consistent with Zhao et al. (Zhao et al., 2023). The  
165 UHPLC-MS/MS equipped with an ACQUITY BEH C18 column (1.7  $\mu\text{m}$ , 100  $\times$  2.1 mm i.d.).  
166 The mobile phase is increased from 5% acetonitrile (A) and 95% ultra-pure water with 0.1%  
167 formic acid (B) at 0 minutes to 95% acetonitrile over 6 minutes, then decreased to 5% A over  
168 0.5 minutes and held for 0.5 minutes. The flow rate was 0.2 mL min<sup>-1</sup> and 2  $\mu\text{L}$  of individual  
169 sample was injected. The column temperature was set at 40°C. The mass spectrometer was  
170 operated in multiple reaction monitoring (MRM) mode. The calculation method for pesticide  
171 mass concentration in ambient air is provided in the Supporting Information (Text S1).

### 172 **2.3 Quality assurance and quality control**

173 To evaluate the accuracy and reliability of the data, laboratory blanks were analyzed following  
174 the same procedure as the samples, and the measured concentrations of the laboratory blank  
175 samples were very low, indicating minimal contamination during processing. The

176 reproducibility of the spiked blanks was acceptable, yielding recoveries ranging from 45.10%  
177  $\pm 3.36\%$  to  $105.3\% \pm 3.29\%$  for gas phase and  $45.40\% \pm 2.64\%$  to  $122.50\% \pm 12.51\%$  for  
178 particulate phase. Except for etoxazole in the gas phase (45.1%) and cyclozaprid and  
179 thiophanate-methyl in the particulate phase (both 45.4%), most pesticides showed good  
180 recovery extracted by dichloromethane and hexane. The average recoveries for 38 pesticides  
181 was  $74.0 \pm 22.5\%$  in the particulate phase and  $73.5 \pm 16.8\%$  in the gas phase. All concentration  
182 data of this study is not adjusted using the recoveries. The limit of detection (LOD) was  
183 estimated as the quantity of analyte with a signal to noise ratio of 3:1, ranging from  $0.01 \text{ pg/m}^3$   
184 to  $9.32 \text{ pg/m}^3$  for gas phase samples and from  $2.22 \times 10^{-4} \text{ pg/m}^3$  to  $5.89 \text{ pg/m}^3$  for particulate  
185 phase samples (Table S4).

## 186 2.4 Gas-particle partitioning models

187 Partitioning of pesticides between the gas phase and particulate phase is often described using  
188 the gas-particle partitioning coefficient ( $K_p$ ,  $\text{m}^3/\mu\text{g}$ ) which defined by Harner and  
189 Bidleman(Harner and Bidleman, 1998):

$$190 \quad K_p = \frac{C_p}{C_g \times C_{TSP}} \quad (1)$$

191 Where  $C_p$  and  $C_g$  are the concentrations of the pesticides ( $\mu\text{g}/\text{m}^3$ ) in the particulate phase and  
192 gas phase, respectively and  $C_{TSP}$  is the concentration of the TSP in the air ( $\mu\text{g}/\text{m}^3$ ).

193 The measured particle-bound fraction ( $\phi_m$ ) can be calculated by the equation(2):

$$194 \quad \phi_m = \frac{C_p}{C_p + C_g} \quad (2)$$

195 [The gas-particle partitioning of soluble organic pollutants in the atmosphere is influenced by](#)

196 [processes such as adsorption, absorption, as well as the removal of particulate matter through](#)  
197 [dry and wet deposition. To examine the dominant partitioning mechanisms, we tested three](#)  
198 [conceptual models, each representing a distinct hypothesis, by simulating relevant gas-particle](#)  
199 [partitioning parameters. For this purpose, we applied three established models that are widely](#)  
200 [used to simulate this process, namely the Junge-Pankow \(J-P\) adsorption model \(Pankow, 1987;](#)  
201 [Iakovides et al., 2022\), Harner-Bidleman \(H-B\) Koa absorption model \(Iakovides et al., 2022;](#)  
202 [Harner and Bidleman, 1998; He and Balasubramanian, 2009\), and L-M-Y model \(Li et al.,](#)  
203 [2015\).](#)

204 The Junge-Pankow (J-P) adsorptive model assumes that the organic matter is adsorbed onto  
205 aerosol surface and relates the predicted particle-bound fraction ( $\phi_p$ ) to [the](#) aerosol surface area  
206 per air volume unit and the saturation vapor pressure of supercooled liquid ( $P_L^0$ , Pa) values  
207 (Pankow, 1987). The  $\phi_p$  can be calculated by the equation (3):

$$208 \quad \phi_p = \frac{c\theta}{c\theta + P_L^0} \quad (3)$$

209 Where  $\phi$  is the fraction of organic matter concentration that is adsorbed onto the aerosol surface.  
210 The parameter  $c$  is a constant with an empirical value of 17.2 Pa/cm.  $\theta$  represents the  
211 contaminated aerosol surface area per unit air volume ( $\text{cm}^2/\text{cm}^3$ ) with a series of representative  
212 values ( $1.0 \times 10^{-7} \text{ cm}^2/\text{cm}^3$  for remote areas,  $1.0 \times 10^{-6} \text{ cm}^2/\text{cm}^3$  for rural areas, and  $1.1 \times 10^{-5}$   
213  $\text{cm}^2/\text{cm}^3$  for urban areas).  $P_L^0$  is subcooled liquid vapor pressure calculated according to the  
214 MPBPVP module in the Estimation Program Interface (EPI) suite (EPIWEB-4.1) of the U.S.  
215 Environmental Protection Agency (U.S.EPA) using the mean temperature (K) during each  
216 sampling period, for the pesticides atrazine, carbendazim, difenoconazole, prochloraz,

217 tebuconazole, hexaconazole, propiconazole, pyrimethanil, and omethoate, the  $P_L^0$  values at  
218 25°C were used as substitutes, since values at the actual temperature were unavailable in this  
219 module (Lohmann et al., 2004).  $\text{Log}P_L^0$  values for the studied pesticides are presented in Table  
220 S5.

221 The Harner-Bidleman (H-B)  $K_{oa}$  absorption model predicts  $K_P$  as a function of  $K_{oa}$  and the  
222 fraction of organic matter in the aerosols ( $f_{om}$ ), assuming that the organic matter is absorbed  
223 into a liquid-like organic film in the particulate matter under the influence of the absorption  
224 force, solubility and particle size (Harner and Bidleman, 1998; He and Balasubramanian, 2009):

$$225 \quad \text{Log } K_P = \text{log } K_{oa} + \text{log } f_{om} - 11.91 \quad (4)$$

226 ~~Where  $f_{om}$  is fraction of organic matter in the aerosols and four  $f_{om}$  values of 5%, 10%, 20% and~~  
227 ~~30% were introduced (Jiang et al., 2020). Here,  $f_{om}$  denotes the fraction of organic matter in~~  
228 ~~aerosols. Four  $f_{om}$  values (5%, 10%, 20% and 30%) were adopted following Jiang et al. (2020),~~  
229 ~~and this range is highly consistent with the measured organic matter fraction of 9% to 41% for~~  
230 ~~aerosols reported by Iakovides et al. (2022). This strong consistency also enhances the~~  
231 ~~credibility of our simulation results.~~  $K_{oa}$  was calculated according to the method in KOAWIN  
232 module of the EPI suite of the U.S.EPA and the equation is as follows (Baskaran et al., 2021):

$$233 \quad K_{oa} = \frac{K_{ow} \cdot RT}{HLC} \quad (5)$$

234 where the  $K_{ow}$  is the octanol-water partition coefficient, with the value at 25°C acquired from  
235 the KOWWIN module in the EPI suite (EPIWEB-4.1) of the U.S.EPA.  $\text{Log}K_{oa}$  values for the  
236 studied pesticides are presented in Table S6.  $R$  is the ideal gas constant ( $\text{Pa mol/K/m}^3$ ) with a  
237 value of 8.314.  $T$  is the mean temperature during each sampling period (K).  $HLC$  is Henry's

238 law constant calculated according to the equation acquired from the HENRYWIN module in  
 239 the EPI suite (EPIWEB-4.1) of the U.S. EPA:

$$240 \quad \ln HLC = A_n - B_n/T \quad (6)$$

241 where T is the mean temperature (K) during each sampling period. The  $A_n$  and  $B_n$  of each  
 242 pesticide are different and the specific values were obtained in the HENRYWIN module.

243 Additionally, the  $\varphi_p$  can be predicted by:

$$244 \quad \varphi_p = 1 / \left\{ 1 + \left[ \frac{1}{(10^{-11.9} \cdot f_{om} \cdot K_{oa}) \cdot TSP} \right] \right\} \quad (7)$$

245 The TSP values for each sampling period were used in this study and the typical values (5%,  
 246 10%, 20% and 30%) of  $f_{om}$  were also inserted.

247 The L-M-Y model was a steady-state model established by Li et al. in 2015, which considered  
 248 the influences of dry and wet depositions of particles and introduced into a non-equilibrium  
 249 parameter caused by dry and wet depositions,  $\log \alpha$  (McEachran Andrew et al., 2015). And the  
 250  $\log K_{P-L-M-Y}$  and  $\varphi_{L-M-Y}$  can be predicted according to the equations (8) and (9) as follows:

$$251 \quad \log K_{P-L-M-Y} = \text{Log } K_{p-H-B} + \log \alpha \quad (8)$$

$$252 \quad \varphi_{L-M-Y} = \frac{K_{p-H-B} \cdot \alpha \cdot TSP}{1 + K_{p-H-B} \cdot \alpha \cdot TSP} \quad (9)$$

253 The  $\text{Log } K_{p-H-B}$  can be calculated by equation (4) and the  $\log \alpha$  can be calculated by

$$254 \quad \text{Log } \alpha = -\text{Log} \left[ 1 + \left( \frac{2.09 \times 10^{-10} f_{om} K_{oa}}{C} \right) \right] \quad (10)$$

255 The values of  $f_{om}$  and the empirical constant C relative to prevailing wind were cited from  
 256 previous studies ( $f_{om} = 5\%, 10\%, 20\%$  and  $30\%$ ,  $C = 5$ ) in the above model (Iakovides et al.,

257 2022).

258 Calculation of RMSE: RMSE for each  $\varphi_p$  of the pesticides detected in the gas phase and the  
259 particulate phase at the same time was calculated to statistically evaluate each partitioning  
260 model and the lower the RMSE value is, the closer is the  $\varphi_p$  to  $\varphi_m$ , indicating that the model has  
261 a better prediction of the gas-particle partitioning of the pesticides in the studied area. The  
262 RMSE can be calculated according to the equation as follows:

$$263 \quad RMSE = \sqrt{\frac{\sum_{i=1}^n (\varphi_{mi} - \varphi_{pi})^2}{N}} \quad (11)$$

264 Where  $\varphi_{mi}$  is the measured particle fraction of each pesticide,  $\varphi_{pi}$  is the particle fraction predicted  
265 by each model, and N is the sample size.

## 266 **3 Results and discussion**

### 267 **3.1 Detection frequency of pesticides in ambient air**

268 A total of 33 pesticides was observed in the gas phase and particulate phase samples of Quzhou  
269 County during the sampling period from February 2023 to May 2023, including 17 fungicides,  
270 12 insecticides, and 4 herbicides. The detection frequencies of these pesticides varied from 7.14 %  
271 (thiacloprid) to 100 % (acetamiprid). The detection frequencies for all quantified pesticides are  
272 given in Table S7. Twenty individual pesticides were detected at least once in both gas and  
273 particle-phase samples, with acetamiprid, imidacloprid, difenoconazole, pymetrozine, and  
274 tebuconazole detected in > 50% samples. Notably, fipronil, a pyrazole insecticide banned in  
275 agricultural production in China since 2009 (Ministry of Agriculture and Rural Affairs of the  
276 People's Republic of China, 2009), was detected in particulate phase samples on March 31st  
277 for the first time and continued to be detected in subsequent particulate phase samples until the

278 end of sampling on May 20th, which might be due to the use of fipronil as sanitary or seed  
279 coating agent of partial dryland crop in the vicinity of the sampling site, as well as its application  
280 in controlling household pests (Cui et al., 2016).

281 Compared with the detection frequencies of pesticides in gas phase (64.29-85.71%), the  
282 detection frequencies in particulate phase were relatively high (71.43-92.86%). The pesticides  
283 of clothianidin, chlorobenzuron, dimethomorph, fipronil, propamocarb, thiophanate-methyl,  
284 tribenuron-methyl, triadimenol, kresoxim-methyl, azoxystrobin, trifloxystrobin and  
285 pyraclostrobin were detected only in the particulate phase.

### 286 **3.2 Concentrations of pesticides in ambient air**

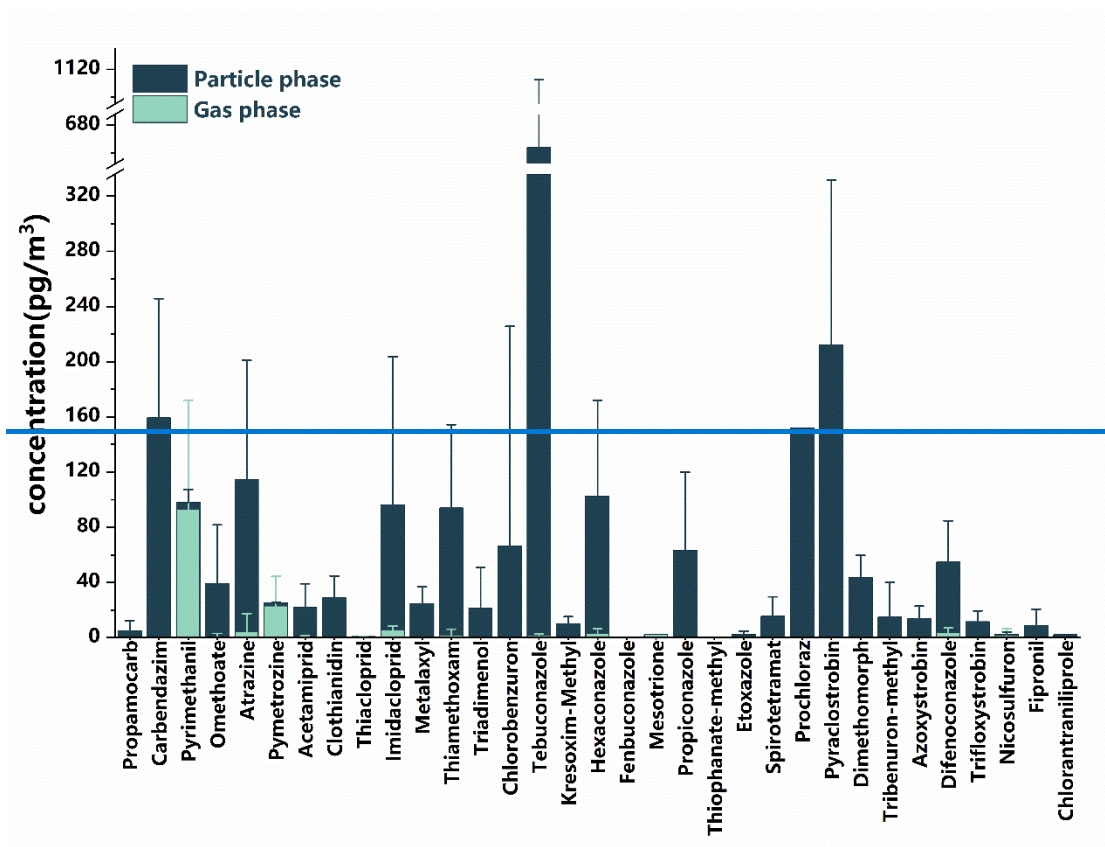
287 In total 33 pesticides were observed with the applied UHPLC-MS/MS method, including 12  
288 insecticides, 4 herbicides and 17 fungicides (Figure 1). The average concentrations of pesticide  
289 in particulate phase ( $2025.76 \pm 1048.83 \text{ pg/m}^3$ ) were significantly higher than  $143.38 \pm$   
290  $146.31 \text{ pg/m}^3$  in gas phase), constituting 93.4% of the total atmospheric pesticide mass. In the  
291 particulate phase, the mean concentration of tebuconazole (a broad-spectrum triazole fungicide)  
292 in the 14 QFF samples was the highest with a value of  $662.49 \text{ pg/m}^3$ , and the mean  
293 concentration of thiophanate-methyl (a thioureas fungicide) was the lowest with a value of  
294  $0.015 \text{ pg/m}^3$ . ~~In the gas phase, pyrimethanil (an aminopyrimidines fungicide) shows the highest~~  
295 ~~average concentration ( $93.00 \mu\text{g/m}^3$ ) in the 14 PUF samples, attributed to its high vapor~~  
296 ~~pressure second only to propamocarb facilitating its volatilization, and the mean~~  
297 ~~concentration of fenbuconazole (a triazole fungicide) was the lowest with a value of  $0.05 \text{ pg/m}^3$ .~~  
298 Among the gas-phase samples, pyrimethanil (an aminopyrimidine fungicide) showed the

299 [highest mean concentration at 93.00  \$\mu\text{g}/\text{m}^3\$  across the 14 PUF samples, attributable to its high](#)  
300 [vapor pressure. In contrast, fenbuconazole \(a triazole fungicide\) with low vapor pressure had](#)  
301 [the lowest mean concentration of only 0.05  \$\text{pg}/\text{m}^3\$ .](#) Research has found that the pesticides in  
302 atmospheric aerosol particles are very persistent because the particles shield the absorbed  
303 compounds from degradation by OH radicals (Socorro et al., 2016). In addition, atrazine,  
304 omethoate and pyrimethanil were detected in samples taken around April 14th and the samples  
305 taken later in the gas phase, probably owing to the application or the fact that with the  
306 temperature raised, there was re-volatilization of this pesticide from contaminated terrestrial  
307 surfaces (Gungormus et al., 2021). Moreover, the pesticide physicochemical properties, their  
308 environmental persistence and the pesticide application technique used may also influence the  
309 atmospheric concentrations of the pesticides (Degrendele et al., 2016). Detailed average  
310 concentration for individual pesticides in the 14 gas-phase and 14 particulate-phase samples  
311 collected during the sampling period from February 2023 to May 2023 are given in Table S8.

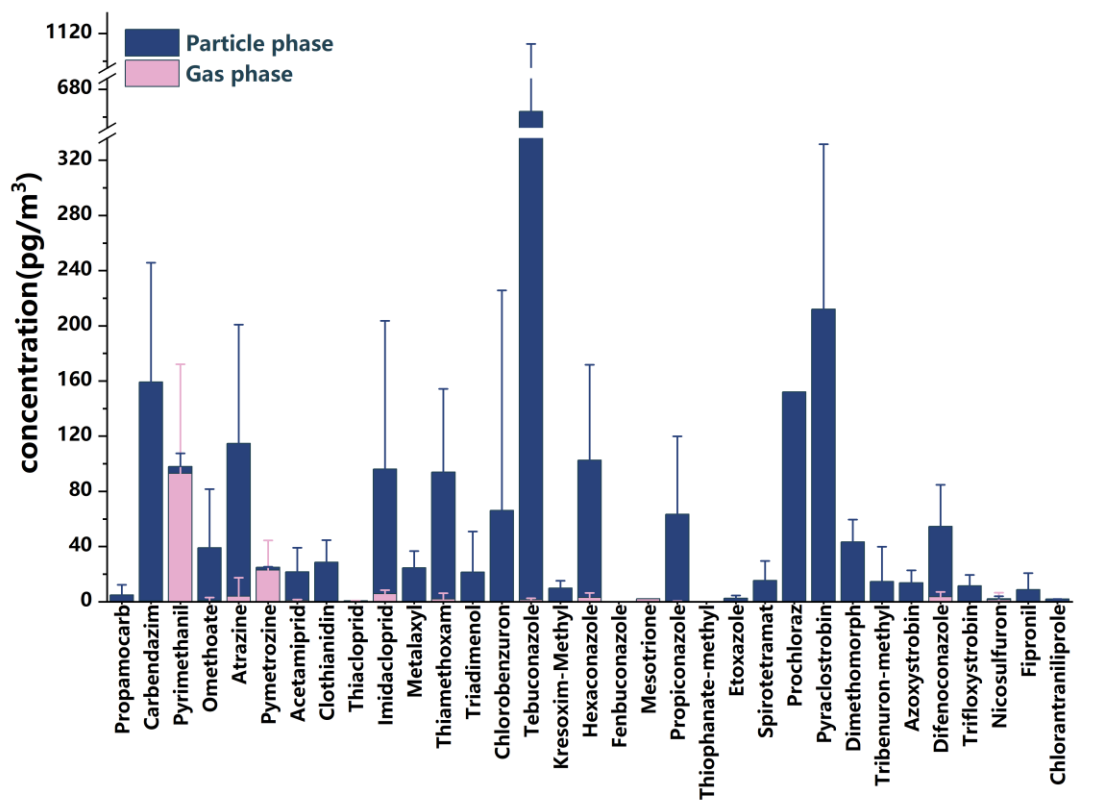
312 Neonicotinoid insecticides (NEOs) stand as the most extensively applied pesticides across  
313 agriculture, boasting versatile applications such as seed dressing, spraying, and soil application  
314 (Zhou et al., 2020). The average concentration of NEOs including acetamiprid, clothianidin,  
315 imidacloprid, thiamethoxam and thiacloprid in atmosphere was 241.18  $\text{pg}/\text{m}^3$ , while it was  
316 232.03  $\text{pg}/\text{m}^3$  for particulate phase and 9.15  $\text{pg}/\text{m}^3$  for gas phase [in our study](#). This is at the same  
317 level as the gaseous pesticides reported by Zhao et al. [\(2023\) from their year-round monitoring](#)  
318 in Quzhou County, the NCP (0.6–26  $\text{pg}/\text{m}^3$ ). In comparison, the average concentration of NEOs  
319 in the particulate phase observed in this study was substantially higher than that associated with  
320  $\text{PM}_{2.5}$  in an urban area of Beijing, China (35.8  $\text{pg}/\text{m}^3$ , [March and October](#)) and nearly three

321 times greater than the PM<sub>2.5</sub>-bound concentration reported for a rural area of Zhengzhou City,  
322 China (80.9 pg/m<sup>3</sup>, [March and October 2019](#)) a conventional agricultural region, as reported by  
323 Zhou et al. (Zhou et al., 2020). Meanwhile, the concentration of individual NEOs for particulate  
324 phase (90.42 pg/m<sup>3</sup>, 20.63 pg/m<sup>3</sup>, 91.82 pg/m<sup>3</sup> and 28.71 pg/m<sup>3</sup> for imidacloprid, acetamiprid,  
325 thiamethoxam and clothianidin, respectively) [in our study](#) was higher than that in the rural area  
326 of Zhengzhou City, China (48.00 pg/m<sup>3</sup>, 17.70 pg/m<sup>3</sup>, 7.20 pg/m<sup>3</sup> and 7.95 pg/m<sup>3</sup>, respectively,  
327 [March and October 2019](#)), probably due to that pesticides observed in our study were in the  
328 TSP samples (including particles with all sizes), whereas the particulate samples in the rural  
329 areas of Zhengzhou City, China were the PM<sub>2.5</sub> fraction. [In a study on the risk assessment of](#)  
330 [airborne agricultural pesticide exposure near fields in the grain-growing area of Liaocheng City,](#)  
331 [China, Hu et al. \(2024\) reported concentrations of acetaminprid, atrazine, imidacloprid, and](#)  
332 [nicosulfuron detected during the sampling period from March to October 2018. The measured](#)  
333 [concentrations were  \$4.88 \times 10^5\$  pg/m<sup>3</sup>,  \$2.17 \times 10^3\$  pg/m<sup>3</sup>,  \$4.11 \times 10^4\$  pg/m<sup>3</sup>, and  \$3.46 \times 10^4\$  pg/m<sup>3</sup>,](#)  
334 [respectively. A study by Hu et al. \(Hu et al., 2024\) on risk assessment of airborne agricultural](#)  
335 [pesticide exposure near the field in the grain growing area in Liaocheng City, China detected](#)  
336 [concentrations of acetaminprid, atrazine, imidacloprid and nicosulfuron at  \$4.88 \times 10^5\$  pg/m<sup>3</sup>,](#)  
337  [\$2.17 \times 10^3\$  pg/m<sup>3</sup>,  \$4.11 \times 10^4\$  pg/m<sup>3</sup>,  \$3.46 \times 10^4\$  pg/m<sup>3</sup>, respectively.](#) The mean concentration of  
338 the above pesticides in our study (21.66 [pg/m<sup>3</sup>](#), 114.72 [pg/m<sup>3</sup>](#), 96.19 [pg/m<sup>3</sup>](#) and 2.17 [pg/m<sup>3</sup>](#)) was  
339 lower than that of the research in Liaocheng City, China, which may be related to the low  
340 pesticide application near the sampling site during the sampling period in this study.

341



342



343

344 Figure 1. The average concentration of individual pesticide in the 14 gas phase (light green)

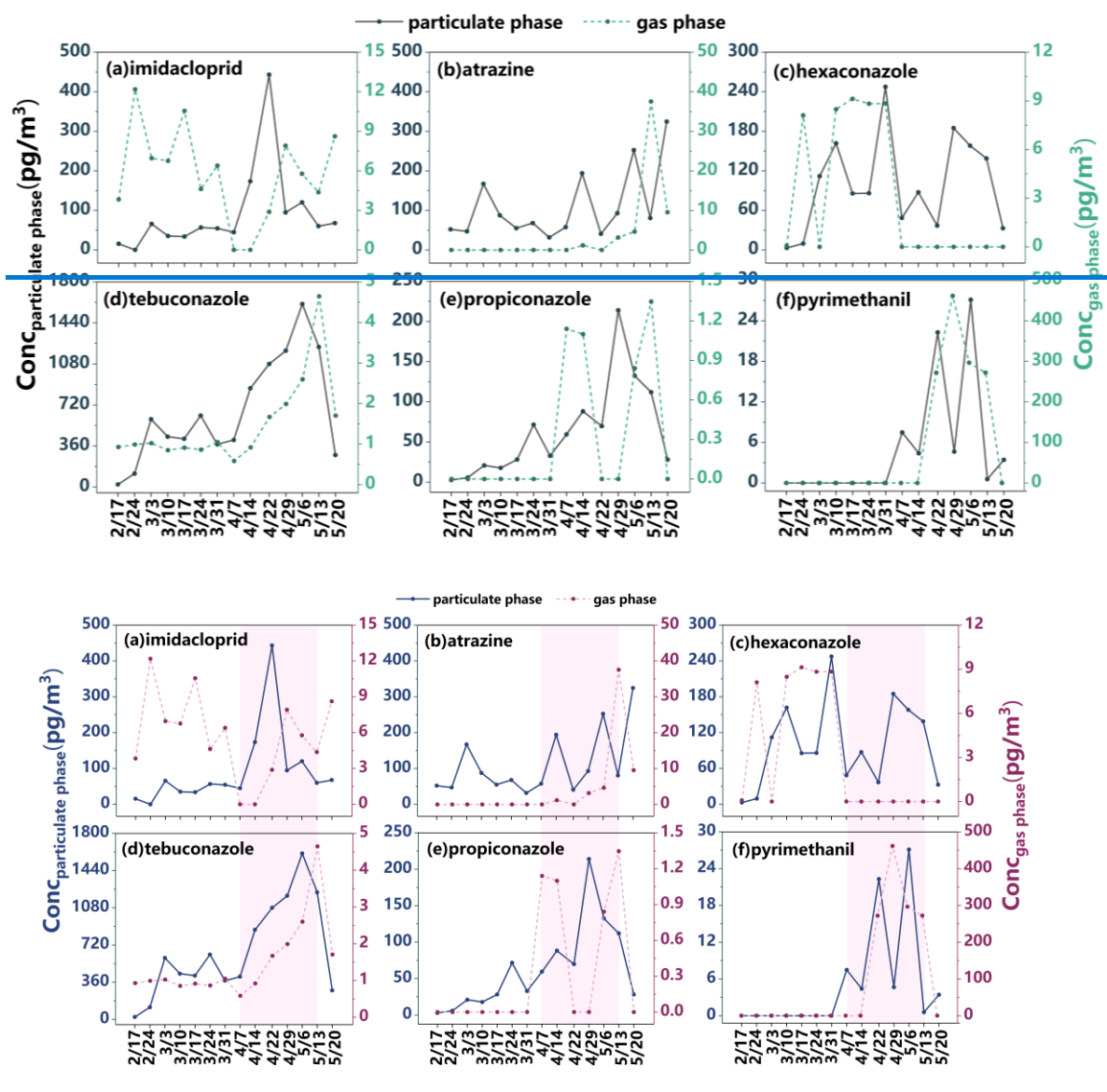
345 and 14 particulate phase (dark green) samples collected during the sampling period from  
346 February 2023 to May 2023. In total 33 pesticides were observed with the applied UHPLC-  
347 MS/MS method.

### 348 **3.3 Temporal variation of pesticide concentration**

349 The concentrations of four typical fungicides (i.e., tebuconazole, prochloraz, pyraclostrobin,  
350 and propiconazole) and the insecticide imidacloprid increased in the particulate phase in mid-  
351 April and early May (Figure 2, Figures S1-S2). In the gas phase, imidacloprid, atrazine,  
352 tebuconazole, and propiconazole showed a similar trend but at lower concentrations than in the  
353 particulate phase, except for pyrimethanil, which had a higher concentration in the gas phase  
354 on April 29th. The concentration of hexaconazole in the gas phase and the particulate phase had  
355 a similar trend over time (Figures S1–S2). This trend aligns with the application timing during  
356 the booting and heading stages of wheat ([early April to mid-May](#)), with peak concentrations  
357 coinciding with pesticide application. In addition, the concentrations of hexaconazole and  
358 imidacloprid in the gas phase were higher than particulate phase before April (the month of  
359 wheat booting stage), this might be caused by the ~~volatilization~~[evaporation](#) of pesticides from  
360 the soil to the atmosphere. Although the temporal distribution patterns of other pesticides in the  
361 gas and particulate phases do not exhibit a high degree of consistency, ~~the concentrations of~~  
362 ~~most pesticides in the particulate phase increased to some extent between mid-April and May~~  
363 ~~(Figures S1–S2).~~[a notable increase in particulate-phase concentrations was observed from](#)  
364 [April to mid-May \(Figures S1–S2\). Notably, this period corresponds to the key pre-harvest](#)  
365 [window for pest and disease control in wheat, which coincides with the booting and heading](#)  
366 [stages \(early April to mid-May\).](#) These findings suggest that pesticide applications near the

367 sampling site resulted in emissions into the atmosphere and subsequent association with  
 368 atmospheric particulate matter. Moreover, the temporal pattern indicates that local sources (e.g.,  
 369 pesticides application in the local fields) dominated atmospheric pesticide concentrations.

370



371

372

373 Figure 2. The concentration trend of different pesticides with sampling dates in particulate phase (full line) and gas  
 374 phase (dotted line) from February 2023 to May 2023. (a) imidacloprid. (b) atrazine. (c) hexaconazole. (d)  
 375 tebuconazole. (e) propiconazole. (f) pyrimethanil. The left coordinate axis represents the concentration of pesticide  
 376 in particulate phase and the right coordinate axis represents the concentration in gas phase. [In the figure, the purple](#)

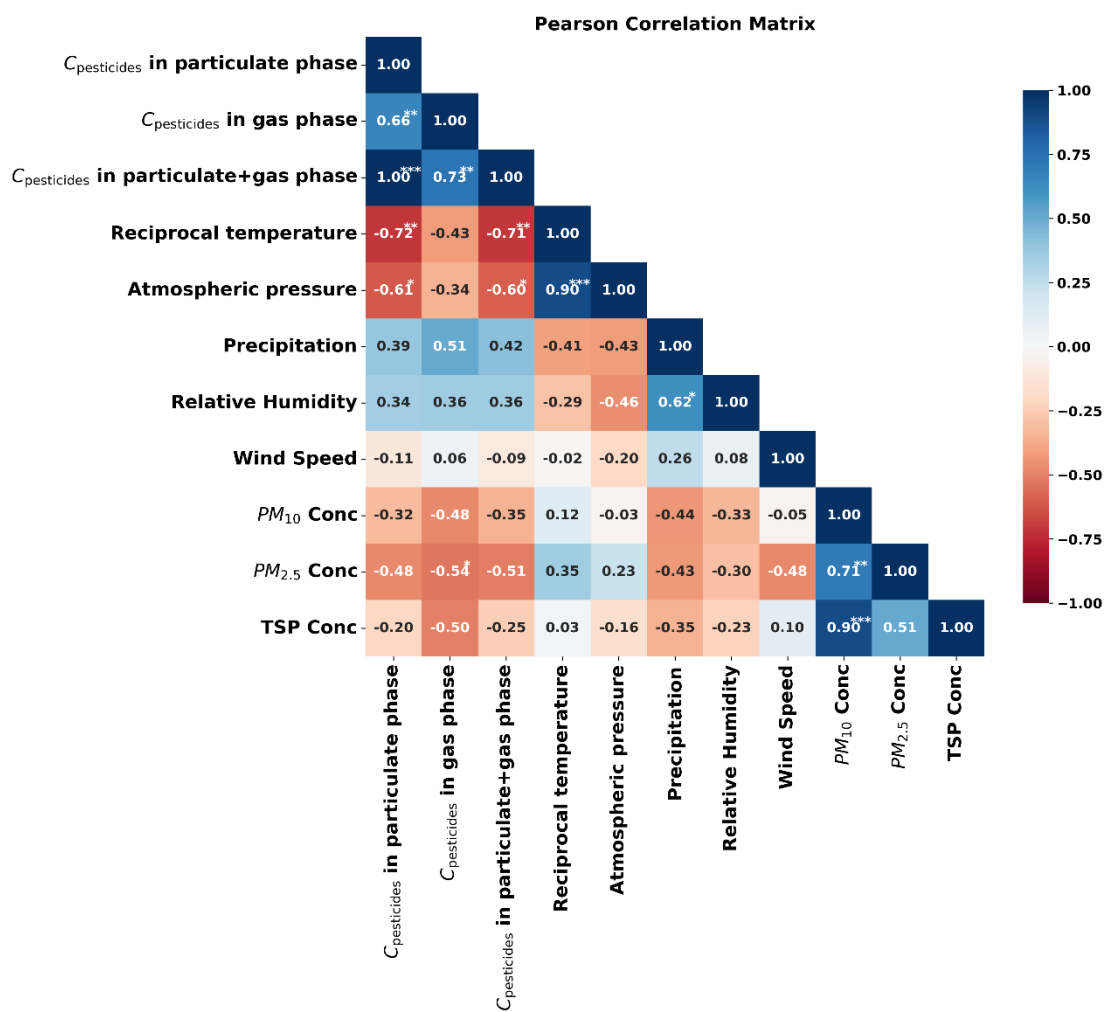
377 [shadow denotes the wheat growth stages from booting to heading.](#)

378

### 379 **3.4 Effect of meteorology on pesticide concentrations in both particulate and gas phase**

380 To elucidate major factors influencing pesticide distribution between the particulate and gas  
381 phases, we used a Pearson correlation matrix to visualize the relationships among total pesticide  
382 concentrations in both phases, meteorological parameters, and particulate matter (PM<sub>10</sub>, PM<sub>2.5</sub>  
383 and TSP) concentrations (Figure 3). A positive correlation with a correlation coefficient of 0.66  
384 ( $p < 0.01$ ) between the particulate and gas-phase pesticide concentrations was observed,  
385 indicating that pesticides in both particulate and gas phase share common sources. A significant  
386 negative correlation was observed between the pesticide concentration in particulate + gas  
387 phase and reciprocal temperature ( $r = -0.71$ ,  $p < 0.01$ ). In other words, rising temperature leads  
388 to an increase of the total concentration of pesticides in the atmosphere, including those in both  
389 gaseous and particulate phases. It can be explained by that more pesticides volatilized from the  
390 soil to the atmosphere with high temperature, which aligns with the finding by Iakovides et al.  
391 ([Iakovides et al., 2022](#)). Figure 3 shows a lack of significant correlation between pesticide  
392 concentrations (both particulate and gaseous) and wind speed, suggesting that the pesticide  
393 concentration in the atmosphere in this study was dominated by local emission sources rather  
394 than long-distance sources by wind. In addition, a significant negative correlation was observed  
395 between reciprocal temperature and pesticide concentration in the particulate phase ( $r = -0.72$ ,  
396  $p < 0.01$ ), whereas no statistically significant correlation was found with the concentration in  
397 the gas phase. Thus, increasing temperatures were connected to an enrichment of pesticides in  
398 the particle phase. This finding is somewhat unexpected, as increased temperatures typically

399 promotes the phase transition of semivolatile organic compounds from the particulate to the  
 400 gaseous phase. [This phenomenon deserves attention and requires further analysis of its](#)  
 401 [underlying causes.](#) Wang et al. (2024) identified temperature as the primary factor influencing  
 402 the gas-particle partitioning of polycyclic aromatic hydrocarbons (PAHs) ~~(Wang et al., 2024).~~  
 403 [This provides a possible explanation, but further verification is needed in our study.](#)  
 404 Atmospheric pesticide concentrations showed no significant correlations with precipitation,  
 405 relative humidity, or wind speed. Negative correlations ( $r = -0.54$  to  $-0.32$ ) were observed  
 406 between pesticide concentrations (in both particulate and gas phases) and levels of  $PM_{10}$  or  
 407  $PM_{2.5}$ .



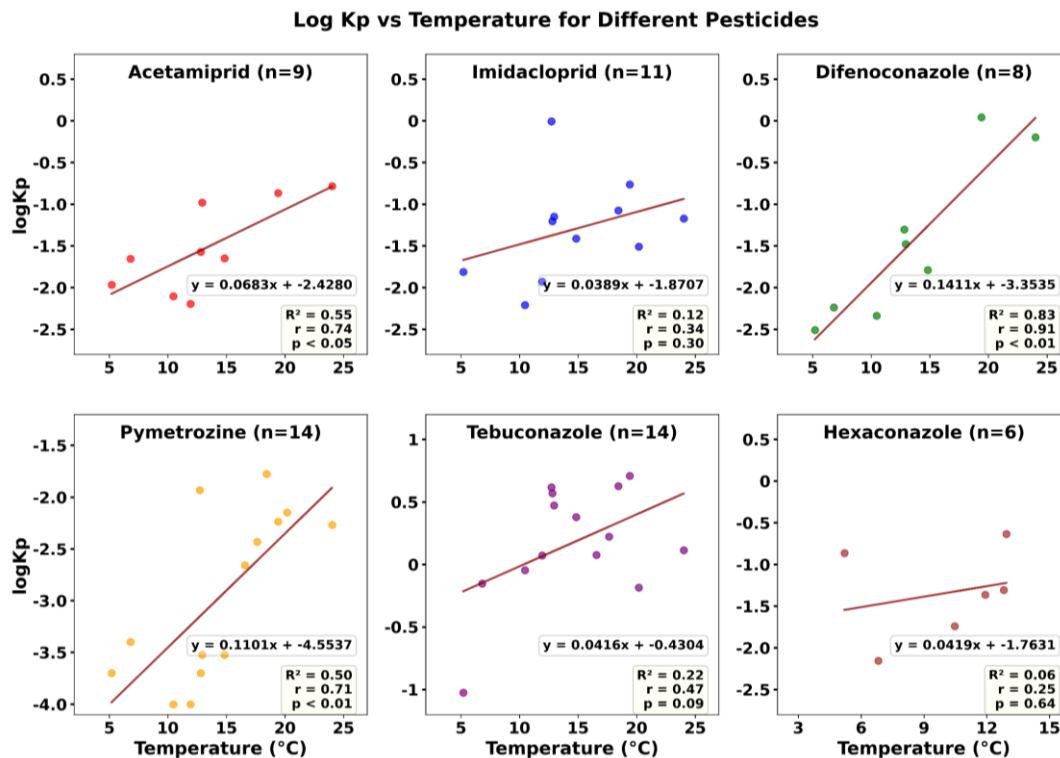
408

409 Figure 3. Pearson correlation matrix of pesticide concentrations in particulate phase, gas phases and particulate+gas  
410 phase with meteorological parameters and particulate matter (PM<sub>10</sub>, PM<sub>2.5</sub> and TSP) concentrations. The values in  
411 the cells represent Pearson correlation coefficients (r). Asterisks indicate statistical significance: \*p < 0.05, \*\*p <  
412 0.01, and \*\*\*p < 0.001.

413 To further investigate the influence of temperature, we performed a correlation analysis  
414 between temperature and the log K<sub>P</sub> values of pesticides meeting the criterion of having more  
415 than five valid data points (i.e., acetamiprid, imidacloprid, difenoconazole, pymetrozine,  
416 tebuconazole, and hexaconazole), as shown in Figure 4. The log K<sub>P</sub> values of all six pesticides  
417 increased with rising temperature. Notably, this correlation was statistically significant for  
418 acetamiprid, difenoconazole, and pymetrozine, indicating that higher temperatures were  
419 associated to their partitioning into the particulate phase. This pattern was mirrored by the  
420 relationship between temperature and the ratio of particulate-phase to gaseous-phase  
421 concentration (C<sub>p</sub>/C<sub>g</sub>) (Figure S4). A study by Zhu et al. in Harbin City, China reported negative  
422 correlations between temperature and log K<sub>P</sub> for most 4–5 ring PAHs, whereas positive  
423 correlations were observed for the 3-ring PAHs (acenaphthylene and acenaphthene) (Zhu et al.,  
424 2021). This contrast highlights the pivotal role of physicochemical properties, which can lead  
425 to completely opposing temperature dependencies for log K<sub>P</sub>. Ulteriorly, the positive correlation  
426 between temperature and the particulate-phase fraction of pesticides, shown in Figure S5, may  
427 be compounded by concurrent increases in relative humidity. Specifically, when temperatures  
428 exceed 290 K, relative humidity is consistently observed to be above 52%. Under these  
429 conditions, elevated humidity can induce a phase transition in particulate matter, decreasing its  
430 viscosity and transforming it into a liquid-like state (Li and Shiraiwa, 2019). This physical

431 change subsequently strengthens the particle's capacity to absorb and retain pesticides.  
 432 Furthermore, agricultural activities (e.g., soil tillage) subsequent to pesticide application in  
 433 spring can accelerate the release of fine soil particles containing pesticides to the atmosphere  
 434 by wind erosion, resulting in the increase of pesticides in the particulate phase (Mayer et al.,  
 435 2024).

436 Therefore, as temperature increased, elevated concentrations of pesticides in the particulate  
 437 phase were observed in this study, accompanied by a rise in log K<sub>p</sub> values. This indicates an  
 438 increase in the C<sub>p</sub>/C<sub>g</sub> ratio with temperature. Pearson correlation and linear regression analyses  
 439 suggest that this trend is likely not governed by a single factor, but rather results from multiple  
 440 interacting drivers, including the physicochemical properties of pesticides, increasing relative  
 441 humidity, the transition of particles to a liquid-like phase, and heightened pesticide application.



442  
 443 Figure 4 The correlation between log K<sub>p</sub> for pesticides and temperature. The "n" in the figure represents the number

444 of valid data points for each type of pesticide in the  $\log K_P$  measurement. Pearson correlation analysis was conducted  
445 between  $\log K_P$  and temperature for pesticides with more than five valid data points.  $R^2$  represents the coefficient  
446 of determination for Pearson correlation,  $r$  represents the correlation coefficient, and  $p$  represents the significance  
447 level.

### 448 **3.5 Gas-Particle partitioning**

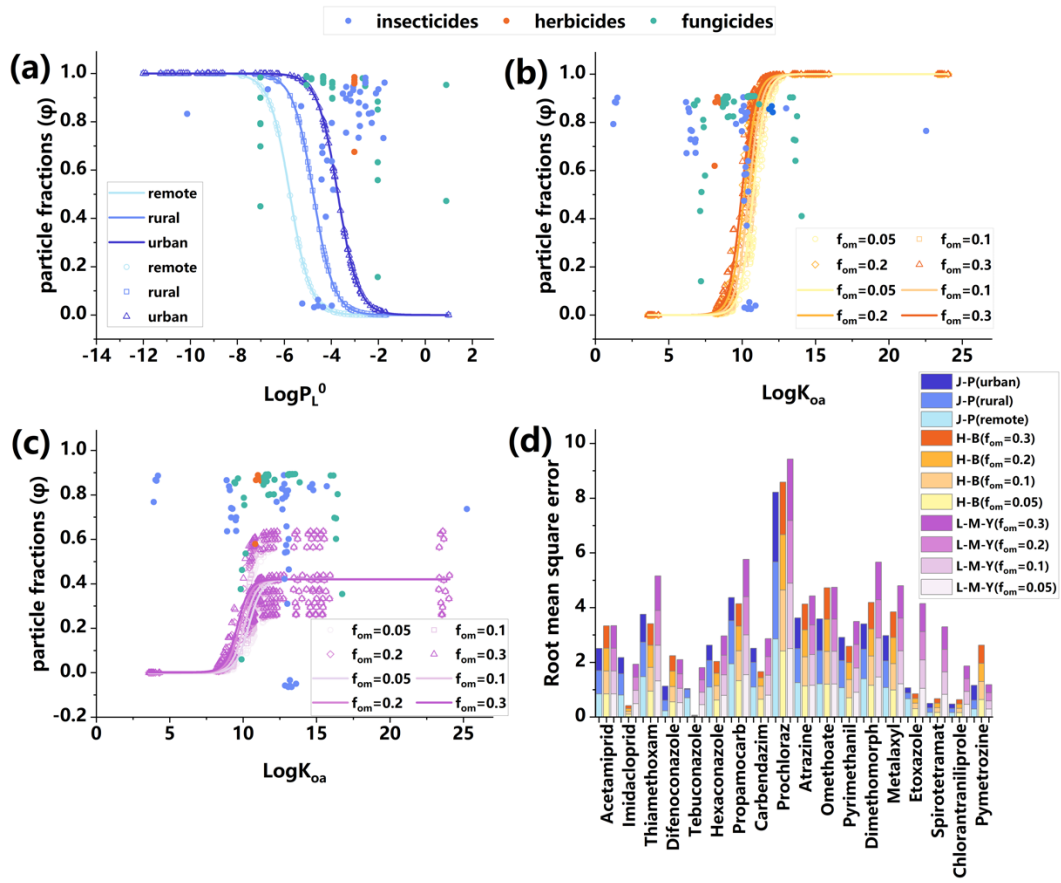
449 ~~In order to investigate the distribution of pesticides in the atmosphere of Quzhou County, the~~  
450 ~~NCP, we analyzed the partitioning of pesticides between the gas phase and the particulate phase.~~  
451 In our study, the gas-particle partitioning coefficient  $K_P$  calculated by equation (1) are  
452 summarized in Table S9. In general, tebuconazole exhibited the highest partition coefficient  
453 ( $K_p$ , 0.09–5.1  $\text{m}^3/\text{pg}$ ) across all sampling periods, indicating a greater tendency for distribution  
454 in the particulate phase, likely due to its low saturation vapor pressure of supercooled liquid  
455 ( $P^{\circ}_L$ ). The  $K_P$  of pymetrozine was markedly low from the February 17<sup>th</sup> to March 31<sup>st</sup> in 2023  
456 and increased significantly from April<sup>7th</sup> to May<sup>20th</sup> in 2023, indicating an approximate tenfold  
457 variation. This phenomenon may be attributed to the progressive partitioning of pymetrozine  
458 into the particulate phase over time. Alternatively, the increased application of pesticides during  
459 the booting and heading stages of wheat could also be a contributing factor. During these stages,  
460 the elevated pesticide usage may lead to emission into the atmosphere, where the pesticides  
461 subsequently bind to atmospheric particulate matter. Other pesticides, including acetamiprid,  
462 imidacloprid and difenoconazole, also showed the same pattern of  $K_P$ . In addition to pesticide  
463 application patterns, an extended sampling duration may lead to the redistribution or  
464 degradation of pesticides during the sampling process itself, which could consequently affect  
465 the measured partition coefficient ( $K_p$ ) values. However, a recent study by Karla et al. (2026)

466 showed that the pesticide concentrations in PUF samplers collected in one week were consistent  
467 with that in three weeks, indicating no significant degradation or diffusion of pesticides in PUF  
468 samplers within three weeks. Therefore, the impact of redistribution and/or degradation process  
469 of pesticides during one-week sampling period on the gas-particle partitioning of pesticides is  
470 very limited.

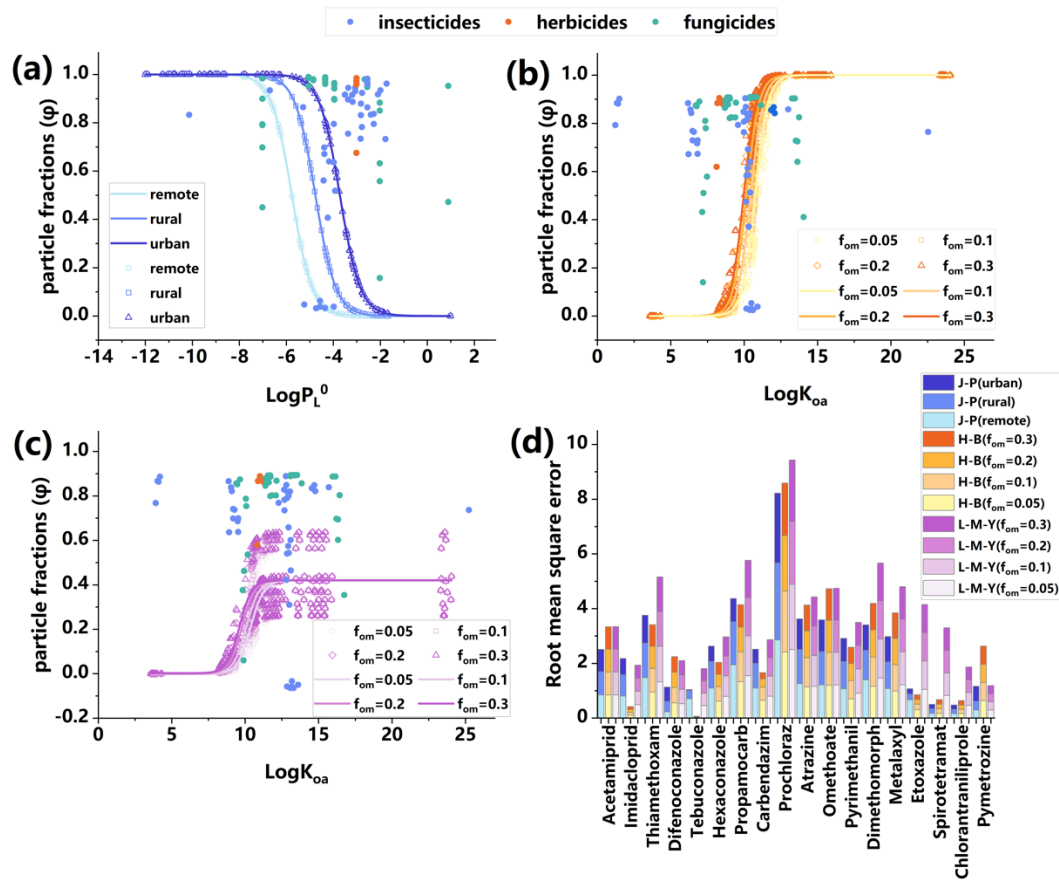
471 Measured particle-bound fraction  $\phi$  of 18 pesticides detected in the gas phase and the particulate  
472 phase were plotted against the corresponding  $P_L^0$  and compared with theoretical curves at given  
473  $\theta$  representing remote, rural and urban areas. Overall, the results presented in Figure 5 show  
474 that most  $\phi$  values ranged from 0.7 to 1, suggesting a potential underestimation of  $\phi$  and  
475 highlighting the limitations of the adsorptive model in accurately simulating  $\phi$  for most  
476 pesticides. This also implies the possible involvement of additional absorption mechanisms  
477 beyond surface adsorption.

478 While gas-particle partitioning models mostly assume thermodynamic equilibrium, kinetic  
479 effects that lead to non-equilibrium states are not captured by the models. Under field conditions,  
480 several factors, such as pesticide source and transport (e.g., drift, volatilization after application  
481 and wind erosion of contaminated soil), the interval between application and sampling, the  
482 distance between application and sampling sites, and environmental conditions, might  
483 significantly affect gas-particle partitioning (Scheyer et al., 2008). Therefore, the  
484 underestimation may be due to pesticides, deposited on soil surfaces, that were resuspended  
485 into the atmosphere by wind erosion, and sampled before gas-particle partitioning reached an  
486 equilibrium state.

487 Furthermore, some uncertainties associated with sampling and analysis methods could also  
488 contribute to differences between theoretical and experimental data. For example, about half of  
489 the  $P_L^0$  values used in predictive models were calculated at 25°C by the U.S.EPA's EPI suite  
490 (v.4.1). In this study, however, samples were collected in winter and spring at temperatures  
491 considerably lower than 25°C (i.e., 0.5–22°C). Considering that  $P_L^0$  of pesticides decreases with  
492 lower temperatures, partitioning into the particulate phase is favored. Consequently, there were  
493 more pesticides distributing in the particulate phase under actual conditions, which caused  
494 higher particle fraction ( $\varphi_m$ ) of each pesticide and underestimation of the model. In addition,  
495 due to the lack of adequate field measurements,  $c$  and  $\theta$  values were estimated from other  
496 studies. Since the constant  $c$  varies for different groups of compounds, the value of 17.2 Pa/cm  
497 may not always be appropriate for each pesticide. The value of  $\theta$  was also affected by the  
498 heterogeneous composition of atmospheric aerosols (contents of organic and elemental carbon),  
499 introducing uncertainty into model predictions. Additionally, the results further confirmed that  
500 the surface area of particulate matter in China may differ from that in Western Europe and the  
501 United States (Fleagle, 1963; Harner and Bidleman, 1998). The air pollution in China is caused  
502 by the production of highly primary emissions and secondary aerosols, while the Great Smog  
503 of London and Los Angeles mainly resulted from coal combustion and photochemical oxidation  
504 of vehicle emissions, respectively (An et al., 2019). Therefore, the actual contaminated TSP  
505 surface area per unit of air volume in Quzhou County should be greater than  $1.1 \times 10^{-5} \text{ cm}^2/\text{cm}^3$ ,  
506 which was used in this model for the urban area.



507



508

509 Figure 5. Measured vs. predicted particle fractions ( $\phi$ ) by applying J-P model (a), H-B model (b) and L-M-Y model

510 (c) for 18 major pesticides detected both in particulate phase and gas phase. (d) The root mean square error (RMSE)

511 of the particle phase fractions of 18 pesticides predicted by the J-P model, H-B model and L-M-Y model. [The empty](#)

512 [dots of different colors represent the predicted  \$\phi\$  values from three models, while the solid dots correspond to the](#)

513 [measured  \$\phi\$  values for various pesticides \(insecticides, herbicides, and fungicides\) examined in this study. The](#)

514 [curves illustrate the predicted trends of  \$\phi\$  values \(represented by empty dots\). In Figure 5\(a\), the line colors indicate](#)

515 [different levels of contaminated aerosol surface area per air volume unit across remote, rural, and urban areas. In](#)

516 [Figures 5\(b\) and 5\(c\), the colors correspond to different fractions of organic matter \( \$f\_{om}\$ \) in the aerosols. The different](#)

517 [colored lines represent remote, rural, and urban areas with different contaminated aerosol surface area per air volume](#)

518 unit and different  $f_{om}$ . The different colored full dots represent different pesticides (i.e., insecticides, herbicides and  
519 fungicides), empty dots represent model prediction  $\phi$  value.

520 In addition to the J-P adsorption model (Figure 5a), measured  $\phi$  particle fractions for 18  
521 pesticides detected in both the particulate phase and gas phase were plotted against their  
522 corresponding  $\log K_{oa}$  values and compared with theoretical partitioning curves at given  $f_{om}$   
523 values (0.05, 0.1, 0.2 and 0.3) based on the H-B absorptive model (Iakovides et al., 2022). As  
524 shown in Figure 5b, the  $\phi$  values predicted by the  $K_{oa}$  absorption model exhibited greater  
525 alignment with theoretical values compared to those predicted by the J-P adsorption model. The  
526 fitting of the pesticides (atrazine, prochloraz, hexaconazole and imidacloprid) with  $\log K_{oa}$  in  
527 the range of 9.98–12.10 was better, with prochloraz and hexaconazole exhibiting the most  
528 precise fitting. This indicates that, compared to the adsorption mechanism, the absorption  
529 mechanism was the main mechanism to describe the gas-particle partitioning of the pesticides,  
530 This might be related to the fact that the increase in temperature causes  $K_{oa}$  to increase (Eq 4),  
531 thereby facilitating the distribution of pesticides into the organic phase, which is consistent with  
532 the previous analysis of influencing factors.

533 For pesticides with  $\log K_{oa}$  values less than 9.98 (omethoate, acetamiprid, propamocarb,  
534 metalaxyl and pyrimethanil), all four prediction curves were significantly underestimated. This  
535 discrepancy can be attributed to the calculation of  $K_{oa}$  values in the model based on the  $K_{ow}$   
536 equation at 25°C, while the samples were collected in winter and spring at temperatures lower  
537 than 25°C. Considering that the  $K_{oa}$  of pesticides increases with the decreasing temperature,  
538 this weakens the trend of the transformation into the gas phase, resulting in more pesticides  
539 distributing in the particulate phase under actual conditions, and caused higher  $\phi$  values.

540 However, for the pesticides with  $\text{Log}K_{oa}$  bigger than 12.10 (difenoconazole, thiamethoxam,  
541 chlorantraniliprole and partial pymetrozine), there was overestimation in all of four curves,  
542 which may be related to the fact that the gas-particle partitioning of these pesticides did not  
543 reach the equilibrium state. Both  $K_{oa}$  and  $P_L^0$  model observations described above imply that  
544 adsorptive and absorptive partitioning are not strong standalone predictors for the pesticides in  
545 the studied atmosphere.

546 Measured  $\phi$  particle fractions for the 18 pesticides mentioned above were also plotted against  
547 their corresponding  $\text{log}K_{oa}$  values and associated with theoretical curves at given  $f_{om}$  values  
548 (0.05, 0.1, 0.2 and 0.3) based on the L-M-Y steady-state model. As shown in Figure 5c, the L-  
549 M-Y model underestimated the distribution in the particulate phase for almost all of the  
550 pesticides, and the fitting performance of the model was inferior to that of the H-B model,  
551 indicating that the distribution of pesticides on particulate matter was closer to the equilibrium  
552 state than that of the steady state. In addition, the farther the distance from the pesticide  
553 application sites to the sampling sites, the higher the proportion of pesticides that distribute in  
554 the particulate phase (Amelia et al., 2005). Therefore, in this model, the underestimation of  $\phi$   
555 values may stem from both local sources and long-range atmospheric transport of pesticides.

556 To better identify the prediction outputs of the three models, the RMSE for each  $\phi_p$  of the  
557 pesticides detected in the gas phase and the particulate phase at the same time was calculated.

558 As shown in Figure 5d, for most of the pesticides, the RMSE values of the L-M-Y model were  
559 higher than those of the other two models, indicating that the L-M-Y model had poorer  
560 predictive performance. The RMSE values of the J-P and H-B models were comparable, with  
561 the H-B model yielding lower RMSE values for 8 pesticides and the J-P model yielding lower

562 RMSE values with 10 pesticides. Although more pesticides fitted with the J-P model achieved  
563 lower RMSE values compared to the H-B model, the mean RMSE value of the H-B model was  
564 lower than that of J-P model, suggesting slightly stronger predictive capability of the H-B model  
565 for  $\varphi$  values.

566 Additionally, the trends of the logarithm of the measured gas-particulate partition coefficient  
567 ( $K_{pm}$ ) to the predicted gas-particulate partition coefficient ( $K_{pp}$ ) and  $K_{oa}$  log-log relationships for  
568 the H-B model and L-M-Y model were also explored and the closer the slope derived from the  
569 fitting line to 0, the better the agreement between  $K_{pm}$  and  $K_{pp}$  and the results are shown in  
570 Figure S3. Compared to the H-B model, the slope of  $\text{Log}K_{pm}/\text{Log}K_{pp}$  and  $\text{Log}K_{oa}$  fitting line  
571 predicted by L-M-Y model was closer to 0, indicating that the L-M-Y model may have better  
572 predictive performance. However, [both two](#) models produced lower  $R^2$ , which might be due to  
573 excessive  $\text{Log}K_{pm}/\text{Log}K_{pp}$  values for individual pesticides (pymetrozine, tebuconazole and  
574 imidacloprid). Therefore, this chapter considers the actual fitting performance of each model  
575 and the results calculated according to RMSE.

576 In general, the  $K_p$  of tebuconazole was the highest in each sampling period, indicating that the  
577 pesticide was more likely to be distributed in particulate phase during the sampling period,  
578 likely due to its low  $P^0_L$ . The  $K_p$  values of pymetrozine, acetamiprid, imidacloprid and  
579 difenoconazole were very low in the first half of the entire sampling period and increased in the  
580 last half of the entire sampling period, owing to the fact that more pesticides distributing into  
581 the particulate phase as time went on or due to an increasing number of pesticides applied in  
582 the fields around sampling site. Compared with the other two models, the H-B model could  
583 better predict the gas-particle partitioning of pesticides in the atmosphere in Quzhou. The

584 absorption mechanism was the main mechanism to describe the partitioning on particulate  
585 matter, but it was not an independent predictor, and other mechanisms were also controlling the  
586 gas-particle partitioning. In addition, the gas-particle partitioning in the atmosphere was closer  
587 to the equilibrium state rather than the steady state, but it still had not reached equilibrium state.  
588 However, field conditions may not be at equilibrium, a possible explanation is that the pollution  
589 in the study area primarily originated from local short-range emissions, as the sampling sites  
590 were located near farmland. High-intensity, close-range emissions could have established  
591 strong concentration gradients in the media surrounding the source, thereby dominating the  
592 short-term atmospheric partitioning behavior of pesticides near our sampling points and driving  
593 it rapidly toward local equilibrium. At the same time, regional atmospheric advection and long-  
594 range transport likely exerted a relatively weak influence given the spatial and temporal scales  
595 of this study. Therefore, although environmental systems are generally open and non-  
596 equilibrium on macroscopic and long-term scales, under specific localized and short-term  
597 conditions, equilibrium models may still serve as effective simulation tools.

#### 598 **4 Limitation**

599 This study has the following two limitations. Firstly, we estimated the gas-particle partitioning  
600 coefficient ( $K_p$ ) using four assumed fractions of organic matter ( $f_{om}$ )—5%, 10%, 20%, and  
601 30%—rather than measured organic matter content. Although the assumed range was informed  
602 by reported organic matter content in particulate matter (9–41%; Iakovides et al., 2022), these  
603 values may still deviate from site-specific conditions. This approach could introduce  
604 uncertainty in predicting pesticide adsorption to the particulate phase. ~~This approach may~~  
605 ~~influence predictions of pesticide adsorption to particulate phases, as adsorption is often~~

606 ~~strongly correlated with organic matter content.~~ In addition, it is also important to note the  
607 limitation imposed by the sampling timeframe (March to May). Seasonal shifts can alter both  
608 pesticide usage and meteorological factors, leading to substantial differences in gas-particle  
609 partitioning across the year. Consequently, the findings may not fully represent year-round  
610 patterns. Future research should include year-round monitoring to address this temporal  
611 variation.

## 612 **5 Conclusions**

613 Utilizing UHPLC-MS/MS method and partitioning prediction models, this study focused on  
614 the gas-particle partitioning of pesticides in Quzhou County, the NCP. Our study demonstrates  
615 that pesticides were predominantly present in the particulate phase, accounting for up to 93.4 %  
616 of the total concentration in the atmosphere. The concentrations of most pesticides in the  
617 particulate phase and gas phase reach the maximum between mid-April and May suggesting  
618 that regional pesticide application patterns drive the temporal concentration trends. It was found  
619 that an increase in temperature significantly promoted the concentration of pesticides in the  
620 atmosphere. Moreover, a positive correlation between temperature and particulate-phase  
621 pesticide concentrations was observed, as indicated by rising  $\log K_p$  values. This pattern is likely  
622 driven by a combination of factors, including pesticide physicochemical properties, ambient  
623 relative humidity, particle phase state and pesticide use patterns. The H-B model could better  
624 predict the gas-particle partitioning of pesticides in the atmosphere, and the absorption  
625 mechanism is the main mechanism to describe the partitioning on particulate matter. In general,  
626 this study indicates that pesticides are mainly absorbed into the internal organic films of  
627 particulate matter in the NCP and advances the understanding of pesticide fate in the

628 atmosphere of the NCP. To further elucidate pesticide behavior in particulate matter, future  
629 study should investigate the occurrence and transformation of pesticides across different  
630 particle size fractions, especially the fine particles.

631

### 632 **Data Availability**

633 The data sets generated in the current study are available at

634 [https://zenodo.org/records/17641894?preview=1&token=eyJhbGciOiJIUzUxMiJ9.eyJpZCI6ImM0ZDAwOWUwLTY4YjAtNGFmMy1iZGFhLWE4YWFjZmE4NDE1ZSIsImRhdGEiOnt9LCJyYW5kb20iOiI2ZDhhMTU4MDc1Zjg4YThjODFiZTk5Zjk0ZTI5OTE2NyJ9.R1](https://zenodo.org/records/17641894?preview=1&token=eyJhbGciOiJIUzUxMiJ9.eyJpZCI6ImM0ZDAwOWUwLTY4YjAtNGFmMy1iZGFhLWE4YWFjZmE4NDE1ZSIsImRhdGEiOnt9LCJyYW5kb20iOiI2ZDhhMTU4MDc1Zjg4YThjODFiZTk5Zjk0ZTI5OTE2NyJ9.R1A8yqr2bWZgp_fe95aDW33pY5MJoF8vFbG8tap-dAiQk9jQJOU_fHWipa8of7cdn0GzqRHyy2-USZeDjk-5VQ)

635 [6ImM0ZDAwOWUwLTY4YjAtNGFmMy1iZGFhLWE4YWFjZmE4NDE1ZSIsImRhdGE](https://zenodo.org/records/17641894?preview=1&token=eyJhbGciOiJIUzUxMiJ9.eyJpZCI6ImM0ZDAwOWUwLTY4YjAtNGFmMy1iZGFhLWE4YWFjZmE4NDE1ZSIsImRhdGEiOnt9LCJyYW5kb20iOiI2ZDhhMTU4MDc1Zjg4YThjODFiZTk5Zjk0ZTI5OTE2NyJ9.R1A8yqr2bWZgp_fe95aDW33pY5MJoF8vFbG8tap-dAiQk9jQJOU_fHWipa8of7cdn0GzqRHyy2-USZeDjk-5VQ)

636 [iOnt9LCJyYW5kb20iOiI2ZDhhMTU4MDc1Zjg4YThjODFiZTk5Zjk0ZTI5OTE2NyJ9.R1](https://zenodo.org/records/17641894?preview=1&token=eyJhbGciOiJIUzUxMiJ9.eyJpZCI6ImM0ZDAwOWUwLTY4YjAtNGFmMy1iZGFhLWE4YWFjZmE4NDE1ZSIsImRhdGEiOnt9LCJyYW5kb20iOiI2ZDhhMTU4MDc1Zjg4YThjODFiZTk5Zjk0ZTI5OTE2NyJ9.R1A8yqr2bWZgp_fe95aDW33pY5MJoF8vFbG8tap-dAiQk9jQJOU_fHWipa8of7cdn0GzqRHyy2-USZeDjk-5VQ)

637 [A8yqr2bWZgp\\_fe95aDW33pY5MJoF8vFbG8tap-](https://zenodo.org/records/17641894?preview=1&token=eyJhbGciOiJIUzUxMiJ9.eyJpZCI6ImM0ZDAwOWUwLTY4YjAtNGFmMy1iZGFhLWE4YWFjZmE4NDE1ZSIsImRhdGEiOnt9LCJyYW5kb20iOiI2ZDhhMTU4MDc1Zjg4YThjODFiZTk5Zjk0ZTI5OTE2NyJ9.R1A8yqr2bWZgp_fe95aDW33pY5MJoF8vFbG8tap-dAiQk9jQJOU_fHWipa8of7cdn0GzqRHyy2-USZeDjk-5VQ)

638 [dAiQk9jQJOU\\_fHWipa8of7cdn0GzqRHyy2-USZeDjk-5VQ](https://zenodo.org/records/17641894?preview=1&token=eyJhbGciOiJIUzUxMiJ9.eyJpZCI6ImM0ZDAwOWUwLTY4YjAtNGFmMy1iZGFhLWE4YWFjZmE4NDE1ZSIsImRhdGEiOnt9LCJyYW5kb20iOiI2ZDhhMTU4MDc1Zjg4YThjODFiZTk5Zjk0ZTI5OTE2NyJ9.R1A8yqr2bWZgp_fe95aDW33pY5MJoF8vFbG8tap-dAiQk9jQJOU_fHWipa8of7cdn0GzqRHyy2-USZeDjk-5VQ) (Guo et al., 2025,

639 <https://doi.org/10.5281/zenodo.17641894>). Figures were made with Matplotlib version 3.8.4

640 (<https://zenodo.org/records/10916799>), available under the Matplotlib license at

641 <https://matplotlib.org/>.

### 642 **Supporting Information**

643 The detailed description of calculation of the mass concentration of pesticides in ambient air

644 (text S1); the trend of different pesticide concentrations in particulate phase with time during

645 the sampling period from February 2023 to May 2023 (Figure S1); the trend of different

646 pesticide concentrations in gas phase with time during the sampling period from February 2023

647 to May 2023 (Figure S2); the slope of  $\text{Log}K_{\text{pm}}/\text{Log}K_{\text{pp}}$  and  $\text{Log}K_{\text{oa}}$  fitting line predicted by L-

648 M-Y model and H-B model (Figure S3); the correlation between  $C_{\text{g}}/C_{\text{p}}$  for pesticides and

649 temperature (Figure S4); the correlation between particulate-phase pesticide concentration and  
650 temperature (Figure S5); the information of the samples (Table S1); the information of the  
651 meteorological data in the sampling period (Table S2); the information of standard substance  
652 (Table S3); the limit of quantitation and limit of detection (Table S4); the  $\log P_L^0$  of each  
653 pesticide in each sampling period (Table S5); the  $\log K_{oa}$  of each pesticide in each sampling  
654 period (Table S6); the detection frequency of the pesticides in gas phase and particulate phase  
655 (Table S7); the concentration of the pesticides in gas phase and particulate phase (Table S8);  
656 the gas-particle partition coefficients of the pesticides (Table S9).

657

#### 658 **Author contributions**

659 Kai Wang contributed in designed the experiments and fundings for this work. Liping Guo was  
660 responsible for data analysis and manuscript preparation. Shuping Shi is responsible for  
661 conducting the experiment. Mingyu Zhao and Hongyu Mu provided guidance for the  
662 experiment. Ying Li provided guidance on the gas-particle partitioning model part. Martin Brüg-  
663 gemann, Daniel M. Figueiredo and Junxue Wu provided guidance on article writing.

664

#### 665 **Competing interests**

666 The authors declare that they have no known competing financial interests or personal  
667 relationships that could have appeared to influence the work reported in this paper.

#### 668 **Acknowledgements**

669 The authors gratefully acknowledge the financial support from the National Natural Science  
670 Foundation of China (No. 42207125 and No. 42475124); Professor Station of China  
671 Agricultural University at Xinzhou Center for Disease Control and Prevention; Mingyu Zhao  
672 acknowledges the China Scholarship Council (No. 201913043).

673 **Financial support**

674 This research has been supported by the National Natural Science Foundation of China (No.  
675 42207125 and No. 42475124), Professor Station of China Agricultural University at Xinzhou  
676 Center for Disease Control and Prevention and the China Scholarship Council (No. 201913043).  
677

678 **References**

- 679 Aktar, M. W., D. Sengupta, and A.: Chowdhury. Impact of pesticides use in agriculture: their benefits  
680 and hazards, *Interdisciplinary toxicology*, 2(1), 1, <http://doi.org/10.2478/v10102-009-0001-7>, 2009.
- 681 Amelia, S, Clymo, Jin, Young, Shin, Britt, A, and Holmén.: Herbicide Sorption to Fine Particulate Matter  
682 Suspended Downwind of Agricultural Operations: Field and Laboratory Investigations, *Environ. Sci.*  
683 *Technol.*, 39(2), 421–430, <http://doi.org/10.1021/es049210s>, 2005.
- 684 An, Z., R. J. Huang, R. Zhang, X. Tie, G. Li, J. Cao, W. Zhou, Z. Shi, Y. Han, and Z. Gu.: Severe haze  
685 in northern China: A synergy of anthropogenic emissions and atmospheric processes, *Proceedings of*  
686 *the National Academy of Sciences of the United States of America*, 116(18), 8657-8666,  
687 <http://doi.org/10.1073/pnas.1900125116>, 2019.
- 688 [Barredo Yera, A. M., Vasconcellos, P. C.: Pesticides in the atmosphere of urban sites with different](https://doi.org/10.1016/j.psep.2021.10.049)  
689 [characteristics, \*Process Saf Environ\*, 156, 559-567, <https://doi.org/10.1016/j.psep.2021.10.049>, 2021.](https://doi.org/10.1016/j.psep.2021.10.049)
- 690 Baskaran, S., Y. D. Lei, and F. Wania.: Reliable Prediction of the Octanol-Air Partition Ratio, *Environ*  
691 *Toxicol Chem*, 40(11), 3166-3180, <http://doi.org/10.1002/etc.5201>, 2021.
- 692 Bedos, C., P. Cellier, R. Calvet, and E. Barriuso.: Occurrence of pesticides in the atmosphere in France,  
693 *Agronomie*, 22(1), 35-49, <http://doi.org/10.1051/agro:2001004>, 2002.
- 694 Brüggemann, M., S. Mayer, D. Brown, A. Terry, J. Rüdiger, and T. Hoffmann.: Measuring pesticides in  
695 the atmosphere: current status, emerging trends and future perspectives, *Environmental Sciences*  
696 *Europe*, 36(1), 39, <http://doi.org/10.1186/s12302-024-00870-4>, 2024.
- 697 Cabrerizo, A., J. Dachs, K. C. Jones, and D. Barceló.: Soil-Air exchange controls on background  
698 atmospheric concentrations of organochlorine pesticides, *Atmos. Chem. Phys.*, 11(24), 12799-12811,  
699 <http://doi.org/10.5194/acp-11-12799-2011>, 2011.
- 700 Cui, J. K., Huang, W. K., Peng, H. Lv, Y., Kong, L. A., Li, H. X., Luo, S.-J., Wang, Y. and Peng, D. L.:  
701 Efficacy Evaluation of Seed-Coating Compounds Against Cereal Cyst Nematodes and Root Lesion  
702 Nematodes on Wheat, *Plant Disease*, 101(3), 428-433, <http://doi.org/10.1094/PDIS-06-16-0862-RE>,  
703 2016.
- 704 Degrendele, C., K. Okonski, L. Melymuk, L. Landlova, P. Kukucka, O. Audy, J. Kohoutek, P. Cupr, and  
705 J. Klanova.: Pesticides in the atmosphere: a comparison of gas-particle partitioning and particle size  
706 distribution of legacy and current-use pesticides, *Atmos. Chem. Phys.*, 16(3), 1531-1544,  
707 <http://doi.org/10.5194/acp-16-1531-2016>, 2016.
- 708 FAO.: Pesticides use and trade – 1990–2023. FAOSTAT Analytical Briefs, No. 109. Rome. ,  
709 <http://doi.org/https://doi.org/10.4060/cd5968en>, 2025.
- 710 Feng, S. J., Xu, W., Cheng, M. M., Ma, Y. X., Wu, L. B., Kang, J. H., Wang, K., Tang, A. H., Jeffrey L.  
711 C J., Fang, Y. T., Keith, G., Liu, X. J., Zhang F. S.: Overlooked Nonagricultural and Wintertime  
712 Agricultural NH<sub>3</sub> Emissions in Quzhou County, North China Plain: Evidence from 15N-Stable  
713 Isotopes, *Environ. Sci. Tech. Let.*, 9(2), 127-133, <http://doi.org/10.1021/acs.estlett.1c00935>, 2022.
- 714 Fleagle, R. G.: Atmospheric processes, *Science*, 140(3567), 653-654,  
715 <http://doi.org/10.1126/science.140.3567.653.b>, 1963.
- 716 Glotfelty, D. E., M. M. Leech, J. Jersey, and A. W. Taylor.: Volatilization and wind erosion of soil surface  
717 applied atrazine, simazine, alachlor, and toxaphene, *Journal of agricultural and food chemistry*, 37(2),  
718 546-551, <http://doi.org/10.1021/jf00086a059>, 1989.
- 719 Gungormus, E., A. Sofuoglu, H. Celik, K. Gedik, M. D. Mulder, G. Lammel, S. C. Sofuoglu, E. Okten,  
720 T. Ugranli, and A. Birgul.: Selected persistent organic pollutants in ambient air in Turkey: Regional  
721 sources and controlling factors, *Environ. Sci. Technol.*, 55(14), 9434-9443,

722 <http://doi.org/10.1021/acs.est.0c06272>, 2021.

723 Guo, L. P., Shi, S. P., Li, Y., M. Brüggemann, Zhao, M. Y., Mu, H. Y., D. M. Figueiredo, Wu, J. X. and  
724 Wang, K.: Gas-particle partitioning of pesticides in the atmosphere of the North China Plain [Dataset],  
725 Zenodo, <https://doi.org/10.5281/zenodo.17641894>, 2025.

726 Harner, T., and T. F. Bidleman.: Octanol– air partition coefficient for describing particle/gas partitioning  
727 of aromatic compounds in urban air, *Environ. Sci. Technol.*, 32(10), 1494-1502,  
728 [http://doi.org/10.1016/S1352-2310\(97\)00013-7](http://doi.org/10.1016/S1352-2310(97)00013-7), 1998. He, J. and R.: Balasubramanian. A study of  
729 gas/particle partitioning of SVOCs in the tropical atmosphere of Southeast Asia, *Atmos. Environ.*,  
730 43(29), 4375-4383, <http://doi.org/10.1016/j.atmosenv.2009.03.055>, 2009.

731 [Hebei Provincial Bureau of Statistics. Hebei statistical yearbook 2024. China Statistics Press. 2024.](#)

732 Hu, Y., Wu, S., Wu, C., Wei, Z., Ning, J. and D. She.: Risk assessment of airborne agricultural pesticide  
733 exposure in humans in rural China, *Environ Geochem Health*, 46(4), 117,  
734 <http://doi.org/10.1007/s10653-024-01882-y>, 2024.

735 Iakovides, M., K. Oikonomou, J. Sciare, and N. Mihalopoulos.: Evidence of stockpile contamination for  
736 legacy polychlorinated biphenyls and organochlorine pesticides in the urban environment of Cyprus  
737 (Eastern Mediterranean): influence of meteorology on air level variability and gas/particle  
738 partitioning based on equilibrium and steady-state models, *J. Hazard. Mater.*, 439, 129544,  
739 <http://doi.org/10.1016/j.jhazmat.2022.129544>, 2022.

740 Jiang, L., Gao, W., Ma, X., Wang, Y., Wang, C., Li, Y., Yang, R., Fu, J., Shi, J., Zhang, Q. H., Wang, Y.  
741 W., Jiang, G. B.: Long-term investigation of the temporal trends and gas/particle partitioning of short-  
742 and medium-chain chlorinated paraffins in ambient air of King George Island, Antarctica, *Environ.*  
743 *Sci. Technol.*, 55(1), 230-239, <http://doi.org/10.1021/acs.est.0c05964>, 2020.

744 [Karla Solano Díaz, Clemens Ruepert, María Melania Ramírez Quesada, Jane A. Hoppin, Frank Wania,  
745 and Berna van Wendel de Joode.: Evaluation of passive air sampling for monitoring Current-Use  
746 Pesticide pollution near large-scale banana plantations in Costa Rica. \*Environ. Sci. Technol.\*, 60 \(4\),  
747 3384-3393, <http://doi.org/10.1021/acs.est.5c11224>, 2026.](#)

748 Kaur, R., G. K. Mavi, S. Raghav, and I. Khan.: Pesticides classification and its impact on environment,  
749 *Int. J. Curr. Microbiol. Appl. Sci*, 8(3), 1889-1897, <http://doi.org/10.20546/ijcmas.2019.803.224>,  
750 2019.

751 Li, Y., and M. Shiraiwa.: Timescales of secondary organic aerosols to reach equilibrium at various  
752 temperatures and relative humidities, *Atmos. Chem. Phys.*, 19(9), 5959-5971,  
753 <http://doi.org/10.5194/acp-19-5959-2019>, 2019.

754 [Li, Y. -F., Ma, W. -L., Yang, M.: Prediction of gas/particle partitioning of polybrominated diphenyl ethers  
755 \(PBDEs\) in global air: A theoretical study, \*Atmos. Chem. Phys.\*, 15\(4\), 1669-1681,  
756 <https://doi.org/10.5194/acp-15-1669-2015>, 2015.](#)

757 Lohmann, R., F. M. Jaward, L. Durham, J. L. Barber, W. Ockenden, K. C. Jones, R. Bruhn, S. Lakaschus,  
758 J. Dachs, and K. Booij.: Potential contamination of shipboard air samples by diffusive emissions of  
759 PCBs and other organic pollutants: Implications and solutions, *Environ. Sci. Technol.*, 38(14), 3965-  
760 3970, <http://doi.org/10.1021/es0350051>, 2004.

761 Mayer, L., C. Degrendele, P. Šenk, J. Kohoutek, P. Příbylová, P. Kukučka, L. Melymuk, A. Durand, S.  
762 Ravier, A. Alastuey, A. R. Baker, U. Baltensperger, K. Baumann-Stanzer, T. Biermann, P. Bohlin-  
763 Nizzetto, D. Ceburnis, S. Conil, C. Couret, A. Degórska, E. Diapouli, S. Eckhardt, K. Eleftheriadis,  
764 G. L. Forster, K. Freier, F. Gheusi, M. I. Gini, H. Hellén, S. Henne, H. Herrmann, A. Holubová Š  
765 mejkalová, U. Hörrak, C. Hüglin, H. Junninen, A. Kristensson, L. Langrene, J. Levula, M. Lothon,

766 E. Ludewig, U. Makkonen, J. Matejovičová, N. Mihalopoulos, V. Mináriková, W. Moche, S. M. Noe,  
767 N. Pérez, T. Petäjä, V. Pont, L. Poulain, E. Quivet, G. Ratz, T. Rehm, S. Reimann, I. Simmons, J. E.  
768 Sonke, M. Sorribas, R. Spoor, D. P. J. Swart, V. Vasilatou, H. Wortham, M. Yela, P. Zampas, C.  
769 Zellweger Fäsi, K. Tørseth, P. Laj, J. Klánová, and G. Lammel.: Widespread Pesticide Distribution  
770 in the European Atmosphere Questions their Degradability in Air, *Environ. Sci. Technol.*, 58(7),  
771 3342-3352, <http://doi.org/10.1021/acs.est.3c08488>, 2024.

772 McEachran Andrew, D., R. Blackwell Brett, J. D. Hanson, J. Wooten Kimberly, D. Mayer Gregory, B.  
773 Cox Stephen, and N. Smith Philip.: Antibiotics, Bacteria, and Antibiotic Resistance Genes: Aerial  
774 Transport from Cattle Feed Yards via Particulate Matter, *Environ. Health Perspect.*, 123(4), 337-343,  
775 <http://doi.org/10.1289/ehp.1408555>, 2015.

776 Ministry of Agriculture and Rural Affairs of the People's Republic of China.: Ministry of Agriculture,  
777 Ministry of Industry and Information Technology, Ministry of Environmental Protection  
778 Announcement No. 1157, edited,  
779 [http://www.moa.gov.cn/nybg/2009/dsanq/201806/t20180606\\_6151221.htm](http://www.moa.gov.cn/nybg/2009/dsanq/201806/t20180606_6151221.htm), 2009.

780 [Mu, H. Y. Zhang, J. C. Yang, X. M., Wang, K., Xu, W., Zhang, H. Y., Liu, X. J., C. J. Ritsema, V. Geissen.:](#)  
781 [Pesticide screening and health risk assessment of residential dust in a rural region of the North China](#)  
782 [Plain, \*Chemosphere\*, 303, 2, <https://doi.org/10.1016/j.chemosphere.2022.135115>, 2022.](#)

783 Ngo, M., K. Pinkerton, S. Freeland, M. Geller, W. Ham, S. Cliff, L. Hopkins, M. Kleeman, U. Kodavanti,  
784 and E. Meharg.: Airborne particles in the San Joaquin Valley may affect human health, *California*  
785 *Agriculture*, 64(1), 12-16, <http://doi.org/10.3733/ca.v064n01p12>, 2010.

786 Pankow, J. F.: Review and comparative analysis of the theories on partitioning between the gas and  
787 aerosol particulate phases in the atmosphere, *Atmospheric Environment*, 21(11), 2275-2283,  
788 [http://doi.org/10.1016/0004-6981\(87\)90363-5](http://doi.org/10.1016/0004-6981(87)90363-5), 1987.

789 Qiao, L. N., Zhang, Z. F., Liu, L. Y., Song, W. W., Ma, W. L., Zhu, N. Z. and Li, Y. F.: Measurement and  
790 modeling the gas/particle partitioning of organochlorine pesticides (OCPs) in atmosphere at low  
791 temperatures, *Sci. Total Environ*, 667, 318-324, <http://doi.org/10.1016/j.scitotenv.2019.02.347>, 2019.

792 Sanlı, G. E., and Y. Tasdemir.: Seasonal variations of organochlorine pesticides (OCPs) in air samples  
793 during day and night periods in Bursa, Turkey, *Atmospheric Pollution Research*, 11(12), 2142-2153,  
794 <http://doi.org/10.1016/j.apr.2020.06.010>, 2020.

795 Scheyer, A., S. Morville, P. Mirabel, and M. Millet.: Gas/particle partitioning of lindane and current-used  
796 pesticides and their relationship with temperature in urban and rural air in Alsace region (east of  
797 France), *Atmos. Environ.*, 42(33), 7695-7705, <http://doi.org/10.1016/j.atmosenv.2008.05.029>, 2008.

798 [Skevas T, Stefanou SE, Oude Lansink A. Pesticide use, environmental spillovers and efficiency: A DEA](#)  
799 [risk-adjusted efficiency approach applied to Dutch arable farming. \*Eur J Oper Res\*, 237\(2\), 658-664,](#)  
800 <https://doi.org/10.1016/j.ejor.2014.01.046>, 2014

801 Socorro, J., A. Durand, B. Temime-Roussel, S. Gligorovski, H. Wortham, and E. Quivet.: The persistence  
802 of pesticides in atmospheric particulate phase: An emerging air quality issue, *Sci. Rep.*, 6(1), 33456,  
803 <http://doi.org/10.1038/srep33456>, 2016.

804 [Sun, H., Chen, H., Yao, L., Chen, J. P., Zhu, Z. H., Wei, Y. Q., Ding, X., Chen, J. M.. Sources and health](#)  
805 [risks of PM2.5-bound polychlorinated biphenyls \(PCBs\) and organochlorine pesticides \(OCPs\) in a](#)  
806 [North China rural area, \*J. Environ. Sci.\*, 95, 240-247, <https://doi.org/10.1016/j.jes.2020.03.051>, 2020.](#)

807 [Tian L, Li J, Zhao S, Tang J, Li J, Guo H, et al. DDT, Chlordane, and Hexachlorobenzene in the Air of](#)  
808 [the Pearl River Delta Revisited: A Tale of Source, History, and Monsoon. \*Environ. Sci. Technol.\*,](#)  
809 [55\(14\): 9740-9749, <http://doi.org/10.1021/acs.est.1c01045>, 2021.](#)

810 Tudi, M., Li, H. R., Li, H. Y., Wang, L., Lyu, J., Yang, L. S., Tong, S. M., Q. J. Yu, H. D. Ruan, and A.  
811 Atabila, D. T. Phung, R. Sadler, and D. Connell.: Exposure routes and health risks associated with  
812 pesticide application, *Toxics*, 10(6), 335, <http://doi.org/10.3390/toxics10060335>, 2022.

813 Turusov, V., V. Rakitsky, and L. Tomatis.: Dichlorodiphenyltrichloroethane (DDT): ubiquity, persistence,  
814 and risks, *Environ. Health Perspect.*, 110(2), 125-128, <http://doi.org/10.1289/ehp.02110125>, 2002.

815 Van den Berg, F., R. Kubiak, W. G. Benjey, M. S. Majewski, S. R. Yates, G. L. Reeves, J. H. Smelt, and  
816 A. M. A. van der Linden.: Emission of Pesticides into the Air, Water, Air, and Soil Pollution, 115(1),  
817 195-218, <http://doi.org/10.1023/A:1005234329622>, 1999.

818 Wang, D. Q., Jia, S. M., Yang, P. F., Zhu, F. J. and Ma, W. L.: Size-resolved gas-particle partitioning of  
819 polycyclic aromatic hydrocarbons in a large temperature range of 50°C, *J. Hazard. Mater.*, 479,  
820 135607, <http://doi.org/https://doi.org/10.1016/j.jhazmat.2024.135607>, 2024.

821 Wang, S. R., A. Salamova, and M. Venier.: Occurrence, Spatial, and Seasonal Variations, and Gas-  
822 Particle Partitioning of Atmospheric Current-Use Pesticides (CUPs) in the Great Lakes Basin,  
823 *Environ. Sci. Technol.*, 55(6), 3539-3548, <http://doi.org/10.1021/acs.est.0c06470>, 2021.

824 Woodrow, J. E., K. A. Gibson, and J. N. Seiber.: Pesticides and related toxicants in the atmosphere,  
825 *Reviews of Environmental Contamination and Toxicology*, 247, 147-196,  
826 [http://doi.org/10.1007/398\\_2018\\_19](http://doi.org/10.1007/398_2018_19), 2019.

827 Yu, B. G., Liu, Y.-M., Chen, X.-X., Cao, W.-Q., Ding, T. B. and Zou, C. Q.: Foliar Zinc Application to  
828 Wheat May Lessen the Zinc Deficiency Burden in Rural Quzhou, China, *Frontiers in Nutrition*, 8,  
829 <http://doi.org/10.3389/fnut.2021.697817>, 2021.

830 Yusà, V., C. Coscollà, W. Mellouki, A. Pastor, and M. De La Guardia.: Sampling and analysis of  
831 pesticides in ambient air, *Journal of Chromatography A*, 1216(15), 2972-2983,  
832 <http://doi.org/10.1016/j.chroma.2009.02.019>, 2009.

833 [Zhao, M. Y., Wu, J. X., D. M. Figueiredo, Zhang, Y., Zou, Z. Y., Cao, Y. X., Li, J. J., Chen, X., Shi, S. P.,](#)  
834 [Wei, Z. Y., Li, J. D., Zhang, H. Y., Zhao, E. C., V. Geissen, C. J. Ritsema, Liu, X. J., Han, J. J. and](#)  
835 [Wang, K.: Spatial-temporal distribution and potential risk of pesticides in ambient air in the North](#)  
836 [China Plain, \*Environ. Int.\*, 182, 108342, <http://doi.org/10.1016/j.envint.2023.108342>, 2023.](#) ~~[Zhao, M.,](#)~~  
837 ~~[Wu, J., D. M. Figueiredo, Zhang, Y., Zou, Z. Y., Cao, Y. X., Li, J. J., Chen, X., Shi, S. P., Wei, Z. Y.,](#)~~  
838 ~~[Li, J. D., Zhang, H. Y., Zhao, E. C., V. Geissen, C. J. Ritsema, Liu, X. J., Han, J. J. and Wang, K.:](#)~~  
839 ~~[Spatial-temporal distribution and potential risk of pesticides in ambient air in the North China Plain,](#)~~  
840 ~~[Environ. Int., 182, 108342, <http://doi.org/10.1016/j.envint.2023.108342>, 2023.](#)~~

841 Zhou, Y., Guo, J. Y., Wang, Z. K., Zhang, B. Y., Sun, Z., Yun, X. and Zhang, J. B.: Levels and inhalation  
842 health risk of neonicotinoid insecticides in fine particulate matter (PM<sub>2.5</sub>) in urban and rural areas  
843 of China, *Environ. Int.*, 142, 105822, <http://doi.org/10.1016/j.envint.2020.105822>, 2020.

844 Zhu, F. J., Ma, W.-L., Liu, L.Y., Zhang, Z. F., Song, W. W., Hu, P. T., Li, W. L., Qiao, L. N. and Fan, H.  
845 Z.: Temporal trends of atmospheric PAHs: Implications for the gas-particle partition, *Atmos. Environ.*,  
846 261, 118595, <http://doi.org/https://doi.org/10.1016/j.atmosenv.2021.118595>, 2021.

847  
848